

## Phenomenology of soil erosion due to rocket exhaust on the Moon and the Mauna Kea lunar test site

Philip T. Metzger,<sup>1</sup> Jacob Smith,<sup>2</sup> and John E. Lane<sup>3</sup>

Received 27 September 2010; revised 11 February 2011; accepted 5 April 2011; published 30 June 2011.

[1] The soil-blowing phenomena observed in the Apollo lunar missions have not previously been described in the literature in sufficient detail to elucidate the physical processes and to support the development of physics-based modeling of the plume effects. In part, this is because previous laboratory experiments have used overly simplistic model soils that fail to produce many of the phenomena seen in lunar landings, some of which therefore went unrecognized. Here, the Apollo descent videos, terrain photography, and ascent videos are interpreted with the assistance of field experiments using a more complex regolith. Rocket thruster firings were performed upon the tephra of a lunar test site on Mauna Kea in Hawaii. This tephra possesses embedded rocks, large fractions of gravel and dust, some cohesion, and natural geological lamination. This produced more realistic plume phenomenology. The relevant phenomena include the relationship of dust liberation with overall soil erosion rate, terrain bed forms created by the plume, dust tails associated with the exhumation and blowing of rocks, bed load transport, the removal of discrete layers of soil hypothesized to be the stratigraphic units corresponding to impact events, the total mass of ejected soil during a landing, and the brightening of the regolith around the landing site. This analysis provides insight into the erosion processes and nature of the regolith. This paper also synthesizes theory, experiment, simulation, and observational data to produce a clearer picture of the physical processes of lunar soil erosion.

**Citation:** Metzger, P. T., J. Smith, and J. E. Lane (2011), Phenomenology of soil erosion due to rocket exhaust on the Moon and the Mauna Kea lunar test site, *J. Geophys. Res.*, 116, E06005, doi:10.1029/2010JE003745.

### 1. Introduction

[2] Several lunar lander missions are presently in the planning stage. Some of these missions do not have rovers and will be investigating the regolith and possibly its content of volatiles directly beneath the lander. It is important for mission success to know how the lander's exhaust plume disturbs the regolith and its volatiles. Also, a number of lunar rover missions are planned as part of the Google Lunar X-Prize competition, including visits to the Apollo sites or other historic sites on the Moon. The blowing spray of soil from their landings could damage those sites and seriously degrade their scientific value as witness plates, surfaces that have sampled the lunar environment for 40 years. During the era of prior lunar landings, the computational power did not exist to enable physics-based simulation to adequately

study and predict the blowing of soil. Now that the computational power exists, the research community still does not understand parts of the physics well enough to develop the software. A series of theoretical, computational, and experimental investigations have been underway to better understand it. Experimental investigations performed on Earth have limited value because it is not possible to fully replicate the lunar environment in sufficiently large scale. For example, to simulate both the vacuum and gravity of the Moon, an experiment must fit inside a vacuum chamber small enough for the cabin of an aircraft flying parabolic trajectories, and at this scale the rocket exhaust gas will fill the vacuum very quickly. Also, there are not any true lunar analog sites on Earth due to the unique nature of lunar soil, which was produced through billions of years of micrometeoroid bombardment. For the space-weathered properties of lunar soil, see, for example, *McKay and Basu* [1983], *Carrier et al.* [1973], *McKay et al.* [1974], *McKay et al.* [1991], *Pieters et al.* [2000], and *Taylor et al.* [2001, 2003]. Ultimately, it is necessary to use theory, simulations, and analysis of the extant lunar data together with lower-fidelity experiments to unravel the physics.

[3] One such experimental investigation was performed in February 2010, when an International team executed a series of lunar technology tests on the volcano Mauna Kea on

<sup>1</sup>Granular Mechanics and Regolith Operations Lab, NASA Kennedy Space Center, Florida, USA.

<sup>2</sup>Pacific International Space Center for Exploration Systems, University of Hawaii at Hilo, Hilo, Hawaii, USA.

<sup>3</sup>ASRC Aerospace, Kennedy Space Center, Florida, USA.

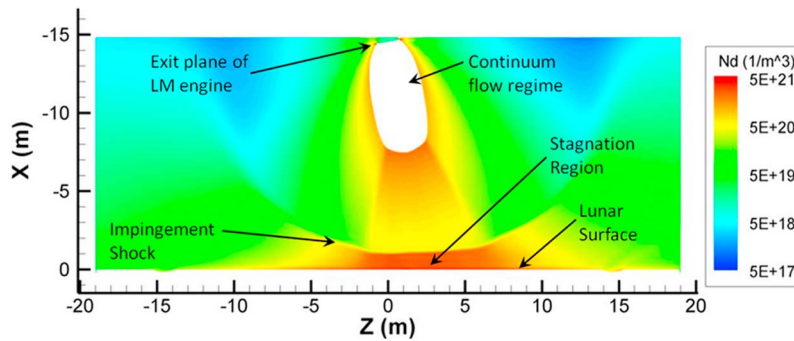


**Figure 1.** Density of the Lunar Module exhaust plume impinging on the lunar surface in numerical simulation. The “continuum flow” volume near the engine nozzle was simulated by a Navier-Stokes solver while the remaining, rarefied volume was by the Direct Simulation Monte Carlo method. Courtesy of F. Lumpkin, NASA Johnson Space Center.

Hawaii Island, Hawaii. The test site was established by the Pacific International Space Center for Exploration Systems (PISCES) because the tephra is chemically adequate to test lunar resource extraction technologies and because nearby geological features would serve to test roving and other lunar surface activities in a harsh environment. One of the major goals of the field campaign was to demonstrate “dust to thrust” in situ resource utilization (ISRU); that is, to demonstrate how oxygen may be extracted from lunar dust (in this case the tephra) and used to generate rocket thrust. The thruster was angled downward onto several surfaces including the tephra and several simulated lunar landing pads to demonstrate how the rocket exhaust plume sand-blasting effect could be mitigated. These experiments should not be interpreted as scaled simulations of lunar landings or a “lunar analog test.” The thruster did not represent a realistic lunar lander engine. The Earth-ambient atmosphere collimated the plume into a narrow jet unlike the lunar vacuum that permits plumes to expand widely. The blowing dust did not run out into vacuum at high velocity but instead ran out into ambient atmosphere and was stopped locally by aerodynamic drag to form billowing clouds. Nevertheless, the tests were valuable because of the poorly sorted character of the soil including embedded rocks, a large fraction of dust and gravel, and natural geological lamination. This was the first terrestrial experiment in which thrusters have been fired upon this type of regolith and it produced several phenomena that have not occurred in prior tests. This shed light on some analogous phenomena in the lunar landings and provided important clues to explain the physics. Also, it produced insights into the relative merits of the various landing pad construction techniques. Furthermore, the high speed videos of these tests will be useful to benchmark the high fidelity fluid/soil physics simulation software packages that are presently being developed through several NASA contracts. This software will simulate plume effects in any environment including the Moon, Mars, or Earth, as well as any scaled testing including small scale in vacuum chambers or tests like those described here. Benchmarking the software with all available data sets will enable us to make more confident extrapolations to environments where there is little access for testing, such as the Moon or Mars.

[4] Terrestrial experiments are most useful when compared to data from the space environment, and the best lunar data for rocket exhaust plume effects to date are the imagery taken during the six Apollo landings, including the landing videos from the Data Acquisition Cameras looking out the pilot’s window (right side) of the Lunar Module (LM), the still photography of the terrain under the LMs after landing, the ascent videos looking out the same window, and the videos of ascent taken by the Lunar Rover Vehicle (LRV) during the final three Apollo missions, along with the flight crews’ verbal descriptions of these effects. When the LMs landed on the Moon, the supersonic plume of rocket exhaust formed a large bowl-shaped shock wave over the surface [Lumpkin *et al.*, 2007; Tosh *et al.*, 2011; Morris *et al.*, 2010] as shown in Figure 1. Directly beneath the nozzle under the shock wave was the stagnation region where the gas was subsonic, dense, and hot. Radially away from the centerline the gas cooled and rarefied as its horizontal velocity increased and became supersonic. The shear stress of the gas upon the soil was very small in the stagnation region due to the low velocity, and it was very small at large distances due to the vanishing density; it was a maximum at some finite radius from the stagnation region on the order of a few meters where neither the velocity nor the density of the gas was very small. The location of this maximum depended on the height of the lander. The gas flow developed a boundary layer over the lunar surface with a velocity gradient related to the local shear stress. The gas picked up soil, lifted it through this boundary layer into the higher velocity gas above the surface, and blew it laterally away at velocities as high as 1 to 3 km/s for the silt-sized particles (4–62.5  $\mu\text{m}$ ) and 0.1 to 1 km/s for sand-sized particles (62.5  $\mu\text{m}$  to 2 mm) according to the most recent estimates [Lane *et al.*, 2008, 2010; Morris *et al.*, 2010]. The erosion rate was controlled by the shear stress [Roberts, 1963; Metzger *et al.*, 2010b] or the turbulent kinetic energy of the gas [Haehnel and Dade, 2008]. The equations by Roberts [1963] indicate that in the annular region where the shear stress was maximum and erosion was taking place the gas was transitional between continuum flow and free molecular flow, meaning that the dimensionless Knudsen number,  $\text{Kn} = \lambda/R$ , was between 0.01 and 1, where  $\lambda$  is the molecular mean free path length

and  $R$  is the radius of a sand-sized grain. This rarefaction affected the viscosity and the spectrum of turbulence and thus the transport of gas momentum through the boundary layer to the soil as well as the drag and lift forces experienced by the individual grains.

[5] At present the erosion rate of soil cannot be predicted under these conditions, which is a critical shortcoming because that determines the amount of damage inflicted by the abrasive sandblasting effect when a spacecraft launches or lands near instruments or other hardware placed on the Moon or other bodies [Clegg *et al.*, 2008; Immer *et al.*, 2011]. Much of the physics of the erosion process is poorly understood even terrestrially, and especially in extreme environments with low gravity, gas that is rarefied and supersonic, and the unusual geological and mechanical properties of lunar or planetary soil. The lunar soil is poorly sorted (has a broad particle size distribution) with a large dust content. It typically has 2 to 20% of the mass smaller than  $10\ \mu\text{m}$  and a median particle size ( $D_{50}$ ) typically near  $50\ \mu\text{m}$ , depending on its maturity [Carrier *et al.*, 1991; Carrier, 2003]. A large quantity of gravel and cobbles are embedded in the soil. It has significant cohesion, due presumably to the Van der Waals force and possibly to non-uniform distribution of electrostatic charge on the particle surfaces [Walton, 2007], both amplified by the large fines content of the soil and the low gravity, plus interlocking particle shapes (the agglutinate particles in the lunar soil being very jagged with concave surfaces) [Carrier *et al.*, 1991]. These have not been adequately characterized for their relative contributions to cohesion in the lunar environment, or for their effect upon Aeolian erosion at the surface of the soil. Most studies of erosion physics have focused on well-sorted, cohesionless sand in subsonic, continuum flow air or water in Earth's gravity [e.g., Bagnold, 1954] and do not include many of the "messy" phenomena of erosion with more complex regoliths described in this paper. Without a better understanding of these phenomena, it will be difficult to interpret data sets obtained from lunar or planetary landings and make progress in elucidating the physics.

[6] Until recently, the aforementioned Apollo data sets have not been utilized to their full potential. Immer *et al.* [2008] recently measured the angular thickness of the blowing dust in the landing videos and found that it is a very thin sheet that is generally no more than 1 to 3 degrees above the lunar surface relative to the impingement point. Metzger *et al.* [2010b] measured the optical density of the dust sheet in the same videos and compared it to small-scale experiments and estimated that several tons of soil were blown during each landing, removing several centimeters of soil over a broad area. There has been very little analysis of the many particular phenomena seen in these videos, however, and almost no analysis of the bed forms on the lunar surface postlanding.

[7] This paper consists of three parts. Section 2 is a new and more detailed description of the phenomena seen during the Apollo landings, the bed forms after landing, and the ascents. Section 3 is the description of phenomena seen in high speed videos and still photography from recent small-scale tests of rocket exhaust blowing on poorly sorted regolith at the field site on Mauna Kea. Section 4 is a discussion

of selected phenomena comparing the field tests with the Apollo landings.

## 2. Phenomena of Apollo Lunar Module Soil Erosion

### 2.1. Apollo Descent Observations

[8] The Apollo mission transcripts and postmission crew debriefings, available in the *Apollo Lunar Surface Journal* (ALSJ) (<http://history.nasa.gov/alsj/>) contain the astronauts' reports of the blowing soil, which they observed during the six Apollo landings. They reported that it was morphologically a thin sheet close to the surface such that rocks often protruded above it or were visible through it [NASA Manned Space Center, 1969b, 1972b]. Aldrin in Apollo 12 noted that the horizon was "obscured by a tan haze" [NASA Manned Space Center, 1969b], which indicated as a lower limit the distance this sheet traveled. The crews reported significant differences in dust density, with Apollo 12 [NASA Manned Space Center, 1969d] and Apollo 15 [NASA Manned Space Center, 1971d] experiencing the densest. J. K. Mitchell [NASA Manned Space Center, 1971b] and H. H. Schmitt (personal communication, 2010) have cautioned that the dust is much brighter and appears optically denser in the descent videos than looking out the windows during landing. This may be a light-integrating and "smearing" effect of the Data Acquisition Camera's shutter speed and film. Even with this effect, Conrad reported that the dust looked much denser out the window in Apollo 12 than it did in the video of Apollo 11 [NASA Manned Space Center, 1969b], which indicated the variability of landing conditions from one mission to the next. The blowing dust was first visible at higher altitudes on the missions that also reported denser dust. It was as high as 100 m (300 feet) and 50 m (150 feet) as reported by Conrad in Apollo 12 and Scott in Apollo 15, respectively [NASA Manned Space Center, 1969d, 1971c, 1971e], and as low as 20–23 m (60–70 feet) as reported by H. H. Schmitt in Apollo 17 [NASA Manned Space Center, 1973]. The plume effects depended on the thrust of the LM (and thus the descent profile). The terminal effects depended on the altitude at which the engine was cut off. These were different on the six landings. A detailed quantitative analysis of the plume effects correlated to the descent profiles is difficult due to the inaccessibility of LM telemetry data, and it is beyond the scope of the present work.

[9] The crews in the six Apollo landings also recorded the plume effects using the Data Acquisition Camera, a 16 mm film camera manufactured by J. A. Maurer Company, which during descent was inside the LM cabin and mounted to look downward through the pilot-side window. It had selectable frame rates of 1, 6, 12, and 24 frames per second (fps) and shutter speeds of 1/60, 1/125, 1/500, and 1/1000 s. The settings during descent varied and for some missions were not documented. The videos were later digitized and converted to 30 fps at the Johnson Space Center (JSC). Quantitative analysis must use methods that are unaffected by the camera settings and digitizing effects, or a detailed study must infer those settings from the extant videos and undo the digitizing effects where necessary. The full resolution digitized videos used in this study were obtained from the JSC video archive. Low resolution versions are available at the ALSJ.

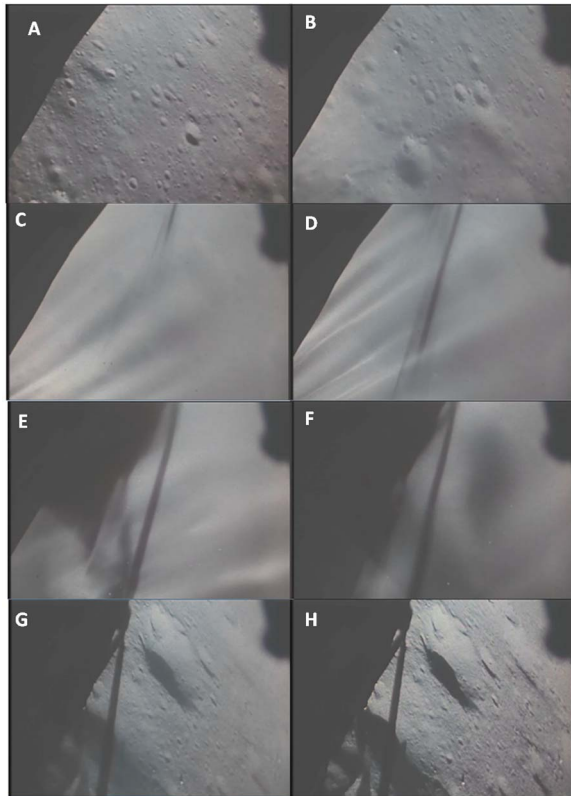


**Figure 2.** Data Acquisition Camera views for Apollo 15, showing the stages of plume/soil interaction: (a) before incipient erosion, (b) smooth flow stage, (c and d) streaking stage, showing increasing structure in the streaks, (e and f) terrain modification stage, showing opaque masses of blowing soil, (g) clearing stage, and (h) after clearing has completed, showing increased contrast and resolution of shadow edges.

[10] Despite the differences between the six landings, their videos demonstrate a core of similar phenomena and can be divided into four stages, which are shown in Figure 2.

[11] First is the smooth flow stage, in which a reduction of contrast or haziness grew within the image of the lunar surface. This is the result of light scattered from a generally homogeneous sheet of dust moving radially away from the impingement point, which was below the lower left corner of the video image. The LM altitude for the onset of this haziness averaged around 30–40 m and indicates the conditions of incipient erosion. Analysis of shadows on the dust sheet [Immer *et al.*, 2008] and simulations of particle trajectories in a simulated lunar rocket exhaust plume [Lane *et al.*, 2008, 2010] agree that the dust sheet was angularly thin in the vertical direction and moved away from the impingement point at an angle of about 1 to 3 degrees above the local terrain.

[12] Second is the streaking stage, in which the haze separated into distinct streaks correlated to specific terrain features. As the lander descended, these streaks became increasingly well defined, more numerous, and narrower. Presumably during the earlier smooth flow stage the plume’s shock had been sufficiently high above the surface and shear stress sufficiently weak such that the boundary

layer was deeper than the hydrodynamic roughness length of the lunar terrain; thus the flow with its suspended dust was smooth [Julien, 1998]. However, as the lander descended the shock became compressed closer to the lunar surface and the shear stress increased [Roberts, 1963], reducing the scale height of the boundary layer until presumably the terrain features were large by comparison, resulting in rough flow and the formation of streaks at each disturbance. As the lander descended further, the flow became rough around smaller terrain features, producing more and narrower streaks. In some landings there was no smooth flow stage, probably because the lander was flying over craters or other features that were large relative to the boundary layer at the height of incipient erosion. Streaks emanated from both the windward and leeward edges of craters as well as from rocks protruding above the soil. They changed their horizontal direction as the lander translated past the terrain features, and the vertical angle of the streaks leaving the surface modulated up and down as the lander’s thrust increased or decreased [Immer *et al.*, 2008]. Toward the end of the streaking stage, as the lander neared the ground, rocks can be seen moving. The rocks flew either above or below the blowing dust sheet in various instances. In at least one case a rock bounced off the lunar surface, but only once within the field of view meaning that its saltation length was very long. At about the same time dust tails began flashing in and out of existence. These were short, bright streaks of dust a few cm wide and 10–20 cm long (order of magnitude), visible beneath the dust sheet and oriented radially away from the impingement point. They appeared suddenly and vanished after about 100 ms. Mitchell (Apollo 14) stated in the ALSJ that the frame rate was set at 24 fps, and the dust tails lasted about three frames in the 30 fps digitized version of that video. Each frame is unique, confirming the camera’s frame rate setting. The dust tails moved a few cm downwind from their original location with each frame before suddenly vanishing. Figure 3 shows eight examples of dust tails during Apollo 14 in six different frames (not sequential).

[13] Third is the terrain modification stage, in which evidently soil was removed by the plume in bulk quantities, not merely as surface erosion. In Apollo 14 and 15, and to a lesser degree in Apollo 17, optically dense and dark, amorphous masses were released suddenly on a large scale, moving away rapidly just before the engine shut off, as illustrated in Figures 2e and 2f. In Apollo 15, rocks blew away visibly during that blast event. In Apollo 12, as shown in Figure 4, two localized “bursts” appeared in the field of view and disintegrated as they traveled away. They released dust streaks that moved faster than the overall bursts, which indicated that the bursts had more inertia and thus were denser quantities of soil than the dust streaks they emitted. In Apollo 11 and 16 the terrain modification stage was less dramatic, but still there were much larger, optically denser dust streaks than during the earlier portions of the descent. Presumably, the plume produced these dramatic ejections of soil in the terrain modification stage because the soil contact probes gouged the lunar surface and created rough, uncompacted areas for the plume gas to break apart; the lander’s legs and footpads protruded down into the boundary layer and disturbed the flow, making it less steady and creating localized regions of enhanced shear stress; the

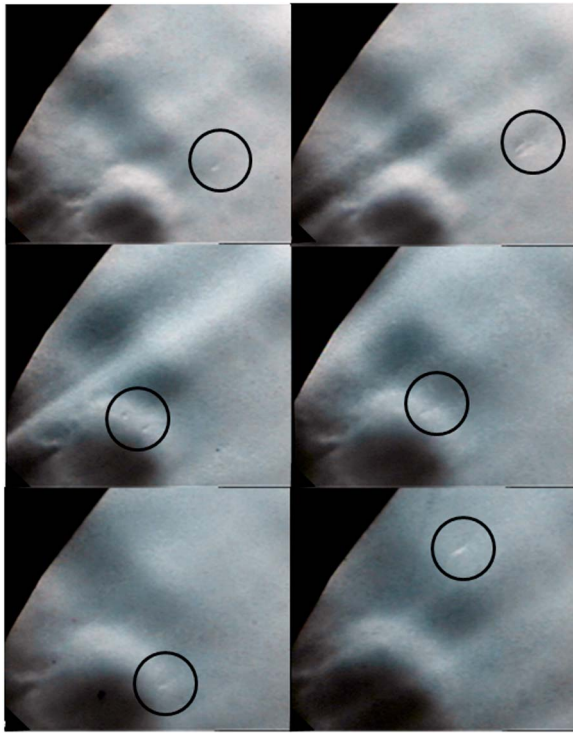


**Figure 3.** Eight dust tails during the Apollo 14 landing. (Two of the circles contain two dust tails, each.)

engine nozzle came very close to the surface creating a more focused stagnation region with sharper pressure gradients that broke up the soil and ejected it; and the footpads impacted the surface with some translational velocity and mechanically broke up the surface. In Apollo 15, which had the largest blast of soil judging by the optical density in the field of view, the engine nozzle buckled upward due to interaction with the ground. Because the nozzle was not in direct contact with the soil after landing, the buckling may have been caused by proximity of the surface causing the gas to choke in the nozzle, producing high static pressure inside [NASA Manned Space Center, 1971e]. It would not be surprising if that event correlates to the largest blast of soil observed in the video, especially if supersonic flow was reestablished causing shock impingement on the soil. The motions of the LM shadows during that blast indicate that the soil was ejected upward at high angles, estimated greater than 22 degrees by *Immer et al.* [2008], not low to the ground like the dust sheet in the smooth flow and streaking stages. During the terrain modification stage the soil may have failed wherever the gas flow was most perturbed and/or wherever the shape of the terrain rendered it the weakest or most exposed. For example, soil on the rims of nearby craters may have blown off en masse.

[14] Fourth is the clearing stage, in which the last of the blown soil traveled away leaving a clear view of the terrain around the LM. In general, some haziness remained or suddenly appeared when the engine was shut off, and it dissipated over the next 10 to 30 s. This haziness may have been dust lifted by the soil depressuring, or it may have been dust lifted by residual electrostatic effects from the charged

plume [Sabaroff, 1965]. On most landings this stage began when the engine was shut off, whether at the time the contact probes first touched the surface (Apollo 12), or later at footpad touchdown (Apollo 11). On Apollo 14, however, the clearing stage began before the crew shut the engine off because they throttled it down and left it operating for several seconds after the vehicle came to rest. During that time the plume continued to generate a single high-velocity dust streak that originated below the field of view of the camera, although the rest of the view cleared normally as the throttled down plume was inadequate to continue erosion where the surface had already been swept clean. The single streak rapidly fluctuated left and right. There is no obvious cause for unsteadiness in the flow to explain this since the LM was stationary on the ground. The only explanation is that the terrain was rapidly changing beneath the vehicle. This streak was probably caused by the localized failure and removal of the uppermost geological unit of the soil as discussed in section 2.2. Thus, in Apollo 14, the moment of engine shutoff was obvious because the streak suddenly disappeared, and at that same moment the burst of haziness appeared in the field of view, decreasing over the next 30 s. The window of the LM is at a considerable height above the surface and the entire field of view was affected by the haziness, so this implies the dust transport mechanism during the clearing stage reached significant heights.

## 2.2. Apollo Postlanding Observations

[15] The astronauts documented the plume effects upon the terrain beneath the LM both orally and photographically. They reported that the engine made no significant crater [NASA Manned Space Center, 1969a, 1969c, 1971b, and

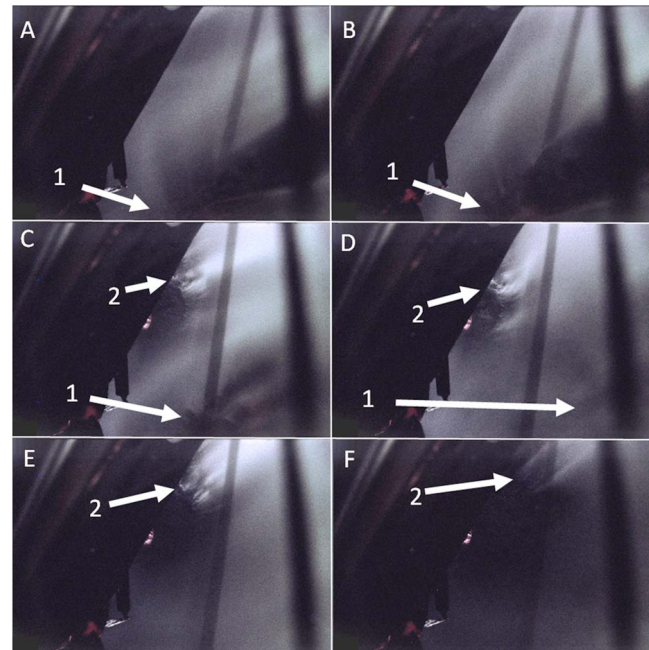


**Figure 4.** In time sequence from Figure 4a to 4f: two localized “bursts” (numbered) seen in Apollo 12 landing, with dust streaks emanating at a higher velocity from the denser bursts.



**Figure 5.** Apollo 16 LRV and flag (NASA photograph A16-107-17438HR). Footsteps and rover tracks darkened the appearance of the soil by mechanical disturbance.

1972a]. However, it swept the surface beneath the LM clean of the loose, noncompacted top layer of the soil [NASA Manned Space Center, 1969c]. Subtle, radial erosion features or “rays” were often evident around the nozzle [NASA Manned Space Center, 1969a, 1971b]. Aldrin (Apollo 11) reported a darkened, “baked” appearance to some of these rays [NASA Manned Space Center, 1969a]. Armstrong (Apollo 11) reported that rocks were disturbed by the plume [NASA Manned Space Center, 1969a]. Bean (Apollo 12) reported that “small, round dirt clods” were dispersed radially [NASA Manned Space Center, 1969d]. Shepard (Apollo 14) reported that the maximum erosion rate was about 1 m (3 feet) southeast of the nozzle rather than directly beneath it [NASA Manned Space Center, 1971b]. H. H. Schmitt (Apollo 17) reported that the engine’s sweeping effects reached as far as 50 m from the LM [NASA Manned Space Center, 1972c]. These observations can be confirmed in the photographs that they took. In the previous analyses [e.g., Scott, 1975], others have discussed the swept appearance beneath the LM: most of the loose material was absent

and thus the top surface of the soil near the LM appeared more densely compacted and smoother than it was further away, while subtle bed forms and markings aligned radially away from the final location of the impingement point (see Figures 9 and 10). Some mechanical disturbance was evident from the interaction of the contact probes and footpads (see Figures 9 and 10). The descending and translating LMs dragged their contact probes through the soil, gouging long, shallow trenches. (These were metal rods designed to bend as the vehicle’s weight bore down toward the lunar surface.) The approximately 1 m (36 in) diameter circular footpads hit the surface oftentimes with significant translational velocity as well as downward velocity, compressing and flattening the soil behind them while mounding up disturbed soil on their leading edges. Both contact probe and footpad interactions indicate the cohesion of the soil: the trenches have vertical sidewalls, and the disturbed soil is in blocky clumps of various sizes up to a couple centimeters in diameter. (Subsequent experiments in the Apollo program, including the digging of trenches and extraction of soil core samples, likewise demonstrated the cohesion and have developed the understanding of soil mechanics much further than this.) The footpads may be the source of some of the dirt clods reported by Bean. Another source is discussed below. Choate *et al.* [1964] reported similar indicators of lunar soil cohesion in the Surveyor program, although in those landings with smaller thrust the surface was not swept entirely clean of the loose material and thus it looked qualitatively different than in the Apollo landings.

[16] Furthermore Scott [1975] noted that a distinct brightening of the soil appeared around the landing sites of the Surveyor spacecraft and LMs. As seen from orbit in Apollo 15, the radius of brightening was roughly 75 m [Hinnert and El-Baz, 1972]. It was also visible to the astronauts on the surface when they drove the Lunar Rover Vehicles (LRVs) some kilometers away from the landing site and looked back. The brightening was apparently no deeper than a thin veneer that lay on top of the darker soil around the spacecraft, because the soil disturbed by astronaut boots or LRV wheels appeared darker, marking the trails of their passage as shown in Figure 5. Scott [1975] interpreted one of these dark “trails,” shown in Figure 6, as the disturbance where the Apollo 12 LM overflowed the soil during its descent. This dark streak does roughly correspond to the trajectory of the LM, but actually it is far too narrow a disturbance to have been caused by the ground track of a

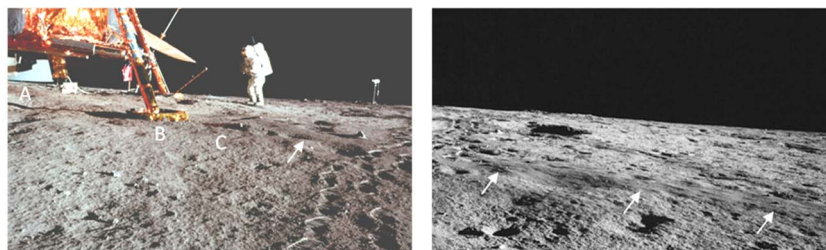


**Figure 6.** Two nearly contiguous photographs showing a dark streak (marked by arrows) oriented radially away from the Apollo 12 LM engine nozzle (A), footpad (B), and contact probe (C). (Details of NASA photographs AS12-46-6779HR and AS12-46-6781HR, contrast enhanced.)

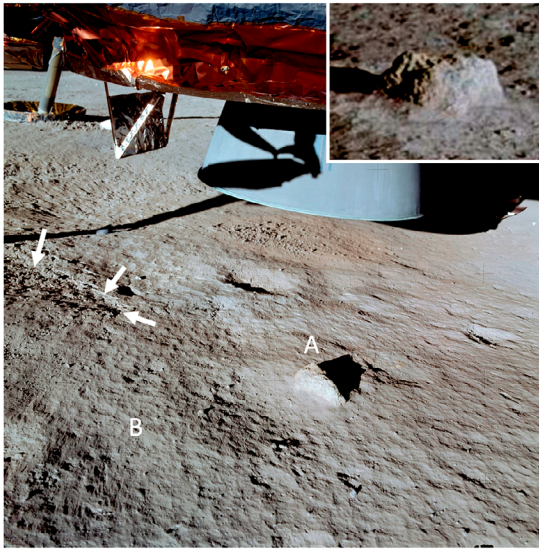


**Figure 7.** Apollo 14 surface (NASA photograph AS14-66-9261HR). Arrows indicate a well-defined contact where the upper soil layer was removed to a consistent depth. Rock A was found beneath nozzle after landing. Surface B has a hummocky texture after being worked by the plume. Inset shows the same rock A from another perspective showing that it is still embedded in the ground. (Detail from NASA photograph AS14-66-9266HR.)

rocket exhaust plume expanding into lunar vacuum. It is along a ray that extends from the engine nozzle through the footpad and soil contact probe. We suggest that it is depositional material and that it stands out from the surrounding terrain because deposition is rare this close to the LM. Plume ejecta were usually lifted by the aerodynamic forces and sent great distances on the order of kilometers to thousands of kilometers [Lane *et al.*, 2008, 2010]. This ray of material was most likely ejected in the terrain modification stage when the soil contact probe broke up the surface. On Apollo 12 the engine was shut down at the first indication of contact from these probes. Hence, the material was part of a bulk release, which would accelerate more slowly than finely dispersed particulates, and the aerodynamic forces were diminishing just as it was released. After nearby deposition along the narrow ray, the material was never subjected to subsequent sweeping of the plume and hence was left with a different texture and photometric function than the surrounding, brighter, plume-swept soil.

[17] Beyond these earlier observed phenomena we offer the following that have not been previously reported. First, there were patches beneath the LM where a distinct layer of soil about a centimeter thick had been stripped away. For example, Figure 7 shows a well-defined contact at the removal of an overlying layer of soil in Apollo 14. The unremoved portions of the upper layer were swept clean, but the freshly exposed surface of the next lower layer was covered by a large number of obstacles (gravel, rocks, and possibly clods) with erosional remnants (ridges parallel to the flow where erosion has been less than the surrounding surface) attached to their downwind sides. These obstacles with their erosional remnants are portions of the overlying

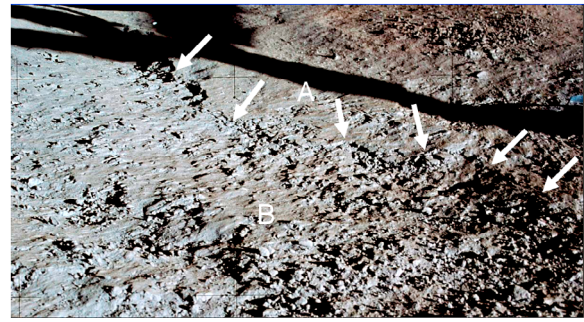


**Figure 8.** Apollo 14 surface showing contact between soil layers where upper layer A was stripped away exposing layer B, on which gravel and/or clumps with erosional remnants lie. (Detail from NASA photograph AS14-66-9267HR, contrast enhanced.)

layer where it had not been completely removed. The thickness of the upper layer all along the length of the contact is consistently about 1 cm, which we estimate using the engine nozzle diameter as the reference. Figure 8 shows the Apollo 14 soil layering from another perspective. Discrete contacts between upper and sub layers were present in the photography for Apollo 11 (shown in Figure 9), 14, and 15. Some well-defined shadows on the soil in Apollo 12 might also represent soil layer contacts. This may have been a source of the clods reported by Bean. In Apollo 16 and 17 there were fewer pictures taken beneath the LM. Thus, the removal of soil in discrete layers appears to have occurred generally, not just in isolated cases.

[18] It is remarkable that this erosion by discrete layers was never identified in the Apollo imagery until now. The most obvious example provided by Apollo 11 (Figure 9) is easily misinterpreted as fissures in a flat surface, possibly



**Figure 9.** Apollo 11 surface. Arrows show the contact between the upper soil layer and the sublayer. Area A has numerous radial erosional remnants, each headed by gravel. Area B has a set of short longitudinal features in the form of downward steps from the impingement point. Trench C was caused by the soil contact probe during landing. The engine nozzle is visible at the top. (Detail from NASA photograph AS11-40-5921HR.)

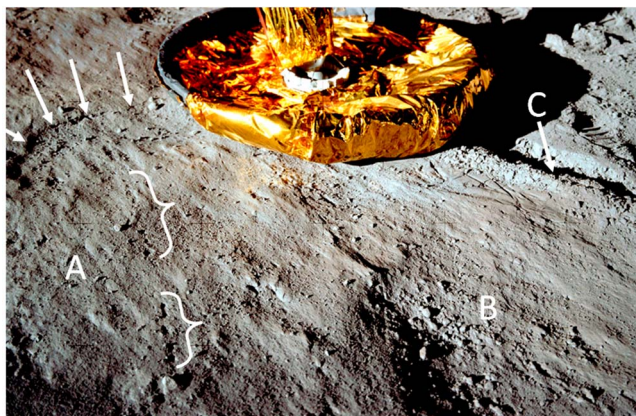


**Figure 10.** Apollo 11 surface showing A, unheaded erosional remnants, B, swath of soil compressed and disturbed by footpad, and C, trench dug by contact probe. Tips of four arrows touch a contact between an upper, partially eroded soil layer and sublayer. The two braces identify a series of skip marks ending at a rock that might have caused them. (Detail from NASA photograph AS11-40-5918HR, contrast enhanced.)

the result of diffused gas eruption [Scott and Ko, 1968], and was interpreted this way by Scott [1975]. Nevertheless, it can be distinguished from fissuring by a close examination of the shadows, which are not consistent with a pair of oppositely facing walls across a narrow gap. It was not until the Mauna Kea field test produced analogous results described in section 3.4 that we were able to see these features as stair steps between sequential layers of soil rather than fissures in a single layer.

[19] Second, at least three types of erosional remnants appear on the lunar surface. In a few places there are erosional remnants that are headed by gravel or rocks and point radially away from the impingement point, but these are surprisingly few. An example is the area marked by A in Figure 9. This is very near to the impingement point, where the radial gas velocity and shear stress are low. It is possible that erosional remnants of this sort could not survive in areas of high shear stress because the embedded gravel was removed quickly while larger rocks that would have remained in place longer were comparatively few. The second type of erosional remnant, as shown in Figure 10, is wider and is not headed by gravel or rocks, but instead rises up with a broad, curved, ill-defined head of soil and points radially away from the impingement point. Perhaps subtle density variations in the soil determined the location of their heads. These can be found further away in areas of high shear stress such as in the vicinity of the footpads. These remnants have a consistent size scale and are estimated to be 2 cm wide, 10 cm long, and only a few millimeters high (within an order of magnitude). By analogy with similar erosional remnants on Earth found in slightly cohesive materials, such as wet sand [Collinson and Thompson, 1989], these features most likely result from the cohesion of the lunar soil and represent a natural symmetry-breaking instability of fluid flow interaction with a cohesive medium.

The third type of erosional remnant is a hummocky texture that does not indicate flow direction, marked as B in Figure 7. The hummocks have a size scale on the order of magnitude of a couple centimeters. Hummocky bed forms on Earth, which are of much larger scale than these under the LMs, have been variously explained as the result of wave action, unidirectional flow, or a combination [Wright, 1993]. Here, we suggest they are the result of the LM translating and exposing the soil to gas flow from different directions, causing the unheaded, radially elongated erosional remnants to be shortened so that their long dimension then matches their short dimension.

[20] Last, several other identifiable but less common features are noted. These include small holes, from which gravel or rocks may have been removed by the plume. Other holes in linear arrangement as in Figure 10 could be skip marks, where a bouncing rock repeatedly struck the surface. These are similar to the series of pits seen on Mars near Viking 1, which were interpreted by Moore *et al.* [1987, see Figure 22B] to be skip marks from an ejected rock. There are also some short longitudinal features or “stair steps” shown marked as B in Figure 9. Judging by their relationship to the eroded contact between soil layers, these are probably contacts of natural soil strata that have been very imperfectly removed. Other than the dark streak shown Figure 6, discussed above, there are no identifiable depositional features, only erosional ones. This is understandable considering the low gravity and the high gas velocity of the plume that resulted in saltation lengths on the order of kilometers to thousands of kilometers [Metzger *et al.*, 2010a].

### 2.3. Apollo Ascent Observations

[21] In the ascent events, analysis of the erosion physics is difficult because there were transient shock effects as the engine ignited, and because the plume impinged on the descent stage (DS) instead of directly on the ground, which complicated the flow field of the gas. The camera view from inside the ascent stage (AS) pilot-side window sometimes looked downward at the terrain (as in Apollo 14 and 16), and other times out toward the horizon (as in Apollo 11 and 15). Sometimes the lighting was too severe and dust could not be seen against the bright lunar surface (as in Apollo 16). Only in Apollo 14 did the internal camera provide useful information on the soil behavior during ascent. On the last three missions, the LRV video camera’s view of the ascent was downlinked to Earth. The LRV was inside the blowing dust and not above it, so it provided information related to the vertical distribution of blowing dust, and this is complementary to the horizontal (radial and azimuthal) distribution seen from inside the AS looking down. The ascent event began with a large burst of debris such as thermal control blankets blown off the DS at high velocity. Much of this material blew upward at high angles (seen by the LRV), but some scudded across the lunar surface and traveled long distances on the order of kilometers (seen from the AS). For Apollo 11, Aldrin reported that they traveled “enormous distances,” while Armstrong reported that “one sizeable piece” traveled one or two minutes before it struck the surface [NASA Manned Space Center, 1969b]. One blanket almost struck the experiment package on Apollo 15 and



**Figure 11.** Supersonic jet (plume) from LOX/CH<sub>4</sub> thruster showing several faint Mach disks (firing at 2500 m altitude on Mauna Kea).

again on Apollo 16 [NASA Manned Space Center, 1972b]. Almost immediately with the blast, dust began to move at ground level (seen by the LRV). The vertical thickness of this dust layer was initially on the order of 10 cm but increased to several meters as the AS rose above the DS and thus more plume gas blew directly onto the soil instead of the DS. The dust distribution was not vertically uniform in this layer, but was more concentrated closer to the surface. There was no well-defined upper limit to the dust layer but instead just a continuing reduction of dust concentration. Seen from the Apollo 14 AS looking down, the blowing dust layer was not horizontally uniform, either, but consisted of several bright, well-defined streaks, plus a number of faint, lesser-defined streaks, upon a very faint amorphous background of blowing dust. The optical density seen by the LRV therefore depended on whether or not it was in a streak, and thus would either overpredict or underpredict the total erosion rate, respectively. The most distinct streaks began below the field of view at or near the DS. Some faint streaks began at terrain features within the field of view, such as the rim of a crater that was several meters in diameter. Bright dust tails occurred on the surface (seen from the AS) and had size, brightness, and duration comparable to those seen in the descent videos. However, a sizable percentage of these, if not all, were (contrary to the descent case) the result of materials breaking off the LM and bouncing off the lunar surface. This mechanically disturbed it, thus releasing the dust that formed the tail. Other plume effects were visible in addition to the regolith disturbances, such as the flag blowing wildly in the Apollo 14 video and airborne debris being redirected by the plume in the LRV videos. Also, O'Brien *et al.* [1970] documented the deposition, due to the Apollo 11 ascent, of dust or debris onto the Dust Detector Experiment (DDE) 17 m way from the LM. O'Brien [2009] quantified for Apollo 12 the existence of collateral dust on the DDE and its subsequent partial removal during AS ascent, though it was 130 m away from the LM. These effects at the DDE could be helpful to benchmark future plume flow codes. It may also be helpful to examine whether any degradation occurred to the LRV video at ascent due to dust impinging on the camera lens, and to examine comprehensively the data from all the instruments

on each Apollo Lunar Surface Experiment Package (ALSEP) to determine whether any other plume effects were detected at ascent.

### 3. Phenomena of Mauna Kea Field Tests

#### 3.1. Background of Field Tests

[22] A number of the plume phenomena observed in the Apollo missions also occurred in the Mauna Kea field tests, and this made it possible to interpret the Apollo plume phenomena. The NASA Johnson Space Center propulsion systems group built and operated the thruster in the Mauna Kea field test as part of the lunar “dust to thrust” demonstration. The thruster used cryogenic oxygen and methane at 2.24 MPa inlet pressure, had a 4.4 mm diameter throat, and produced nominally 72 N thrust. The resultant plume was observed to be supersonic as indicated by the Mach disks in Figure 11. Although the thrust was small, the Earth-ambient atmosphere collimated it into a narrow jet with a high shock recovery pressure when impinging on the surface of the soil. This jet would therefore have excavated a deep, narrow hole in the soil, similar to that of a “posthole digger,” through bearing capacity failure [Alexander *et al.*, 1966] and/or diffusion-driven shearing [Metzger *et al.*, 2009a, 2009b]. This would be unrepresentative of the plume effects seen in the Apollo lunar landings. Because of the mechanical competence of the lunar soil's sub layer, the high thrust of the LM did not create deep craters. To avoid deep cratering in the Mauna Kea field tests and ensure the physics would be in the same surface erosional regime as in Apollo, the test team adjusted the height and tilt of the thruster above the soil until its potential core no longer reached the surface. This showed the length of the potential core to be less than a meter and so the thruster was pointed at  $\alpha = 52.2$  degrees angle relative to the vertical with its exit plane at  $y = 38.9$  cm above the ground. The slant distance along its centerline to the ground was  $L = y/\cos(\alpha) = 63.5$  cm.

#### 3.2. Field Test Soil Properties

[23] The soil at the field test site consisted of fine-grained volcanic tephra that was located in a modern natural drainage wash at 2500 m altitude on the southern slopes of Mauna Kea. We measured the specific gravity of the

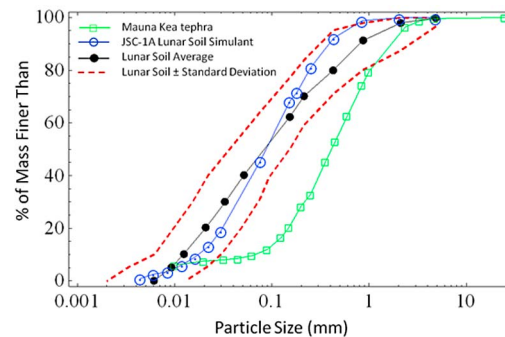


**Figure 12.** Particle size distribution of test site tephra compared to lunar soil and JSC-1A lunar soil simulant. Lunar and JSC-1A data courtesy of Xiangwu Zeng, Case Western Reserve University [Zeng *et al.*, 2010].



**Figure 13.** Vibrational hand compactor used to densify the tephra.

material and found it to be 2.34, which is lower than the range of specific gravities 2.9 to 3.5 measured for lunar soil samples by *Carrier et al.* [1991]. Our measurement was made in water so intragrain micropores would not have been wetted. Thus 2.34 should be interpreted as a “grain-average” specific gravity, which is appropriate to predicting the aerodynamic behaviors of the grains. The particle size distribution of the tephra was found by standard dry and wet sieving and is shown in Figure 12 in comparison to lunar soil simulant JSC-1A, which was measured by *Zeng et al.* [2010], and lunar soil, which was measured by *Carrier et al.* [1991] and *Carrier* [2003]. Although the Mauna Kea tephra is significantly coarser than lunar soil, deficient in silt and fine sand while having an abundance of coarse sand, it does have a dust fraction  $<10 \mu\text{m}$  within the range of lunar soil. It is this dust fraction that dominates the optical density as discussed below and thus the visible phenomenology in the recorded videos.

[24] We subjected several soil preparations to the thruster firings: (1) unmodified, natural tephra; (2) tephra graded such that the looser material in the top 20 cm was removed by a remotely controlled lunar excavator and/or by a handheld aluminum plate, thus exposing the more competent sub layer of tephra; (3) tephra that was graded to the same 20 cm depth followed by vibrational compaction; and (4) tephra that was graded, vibrationally compacted, and then tamped. We performed vibrational compaction with a Kompax Vibratory Compaction Plate (hand compactor) model VCP110, shown in Figure 13. We performed tamping by dropping a standard 5.3 kg sledge hammer from a height

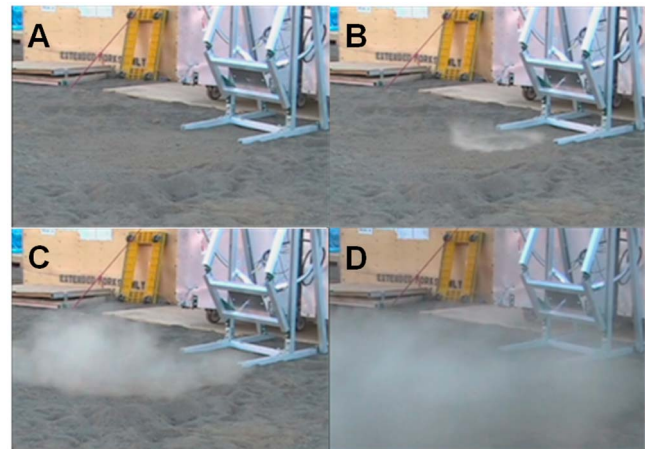


**Figure 14.** Typical thruster firing. (a) Before ignition. (b) Splash stage. (c) Advection stage. (d) Clearing stage.

of about 10 cm onto a thick,  $30 \times 15$  cm aluminum plate lying on the surface of the soil. We performed 4 to 6 tamps in each area and then moved the plate to a new area of the soil. Nine thruster firings were performed on these surfaces as listed in Table 1.

### 3.3. Test Results for Baseline (Cases 1 and 2)

[25] The progression of a typical thruster firing is shown in Figure 14. The event can be conveniently divided into three stages. We describe these in detail for cases 1 and 2 to serve as the baseline for comparison with the other cases.

[26] First is the splash stage. Immediately after ignition, the subsonic, turbulent gas from the jet abruptly impinged upon the ground causing a splash. This consisted of an annular ring of brightly illuminated, optically dense dust around the impingement point as shown in Figure 15. It was nonhomogenous, with dense streaks and billows in some areas, and dust-free patches elsewhere due to the unevenness of the terrain. In the videos, there was no visible motion of larger sand-sized or gravel-sized particles associated with the initial dust lifting. It may be that sand-sized particles were already moving, but they were not visible, as discussed below. There was no splash stage in the Apollo landings because the gas density over the soil built up slowly as the lander descended. The LM ascent events included the

**Table 1.** Test Cases for Thruster Firings

Test Case	Soil Type	Comments
1	Unmodified	Includes rocks and loose gravel
2	Unmodified	Second firing on surface of case 1
3	Unmodified	Small “craters” added to surface of case 1
4	Unmodified	Larger “craters” added to surface of case 1
5	Disturbed then vibrated	Grading process disturbed it excessively prior to compacting by vibration.
6	Disturbed then vibrated and tamped	Same surface as case 5 but recompacted by additional vibration plus tamping
7	Graded, only	Probably had remnant moisture
8	Graded, only	Same surface as case 7
9	Graded then disturbed	Same surface as cases 7 and 8 but broken up and loosened by hand (see text)

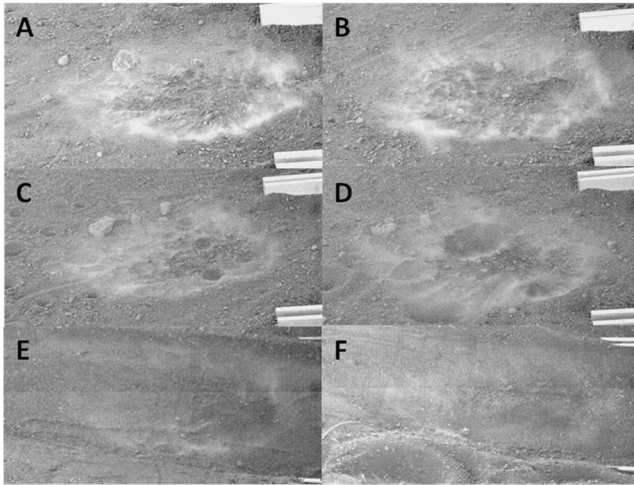


**Figure 15.** Splash stage: dust ring raised around impingement point at thruster ignition. (a–d) Test cases 1 through 4 using unmodified soil. (e) Test case 5 using vibrationally compacted soil. (f) Test case 6 using vibrationally compacted and tamped soil.

analogy of the splash stage, but there was no visible dust ring because the imaging failed to capture it or the DS broke up the plume so that it struck the surface less coherently than in the field tests. A vehicle launching directly off the lunar surface (no DS left behind) would have a dramatic splash stage.

[27] Second is the advection stage. The dust ring expanded outwardly as more dust was continually generated at the original radius of the ring and beyond. Both radial and annular structures could be seen in the suspended, advecting dust, as illustrated in Figure 16. The radial structures (streaks), which could be either quasi-static or rapidly varying, emanated from areas of enhanced erosion such as ridges, craters, or rocks that were being undercut. The enhanced dust release from ridges usually ended very quickly, probably because the bulk soil forming the ridge had already blown away. The annular structures in the suspended dust appeared as arc-shaped waves that propagated outwardly in rapid succession. They were due to the unsteadiness of the turbulent end of the jet in the ambient atmosphere causing a cyclical variation in the erosion rate. The Apollo plumes did not create annular structures in the dust, and this confirms the expectation that the impinging Apollo plumes were steady. Also during this stage, the gravel-sized particles began to move. While the dust-sized particles were in suspension, the gravel-sized particles rolled and bounced along the surface as bed load. Some gravel particles were seen on high ballistic trajectories as they ricocheted off surface features such as embedded cobbles. In all directions the rolling bed load moved at much lower velocity than the suspended dust. All transport (suspended and bed load) was primarily downstream away from the jet (because it impinged the soil at the sharp angle  $\alpha$ ) with only a little back flow along the ground toward the test rig. Thus, canting the nozzle appeared to be an effective method to control the direction of the spray (at least in an atmosphere and when there was no deep crater formation). During this stage, bright dust tails formed in the wake of some of the

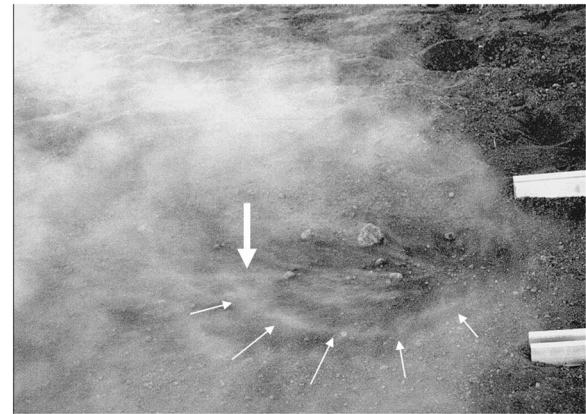


**Figure 16.** Advection stage. Wide arrow indicates a typical radial dust streak. Thin arrows indicate a typical annular structure in the blowing dust.

gravel and cobbles, some that were bouncing away (when they had enough mass to disturb dust with each bounce) and some that were still partially embedded in the soil. Obstacle scour occurred around the embedded ones until the removal of soil exposed enough of their surfaces to the dynamic pressure of the gas flow and they were torqued up and out from their resting places in the soil and rolled away. This left holes in the soil behind them, which seemed to rapidly disappear, being filled by deposition of sand, or erased by the lowering of the surface around them via erosion, or by a combination of both. The sustained dust tails that formed in the wake of embedded rocks did so during this exhumation process, as shown in Figure 17. This stage is analogous to the streaking stage of the Apollo landings. In the field tests there was no analogy to the amorphous stage of the Apollo landings because the jet was always close to the surface and the boundary layer was always shallow relative to the surface roughness.

[28] Third is the clearing stage. After the thruster shut off, the bed load transport of gravel ended quickly, but the suspended dust cloud slowly drifted away with the ambient

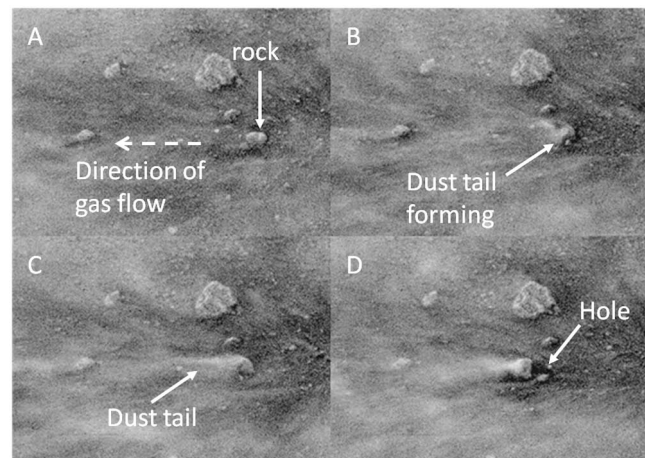


**Figure 17.** Exhumation of a rock showing the formation of a dust tail just before the rock moves.

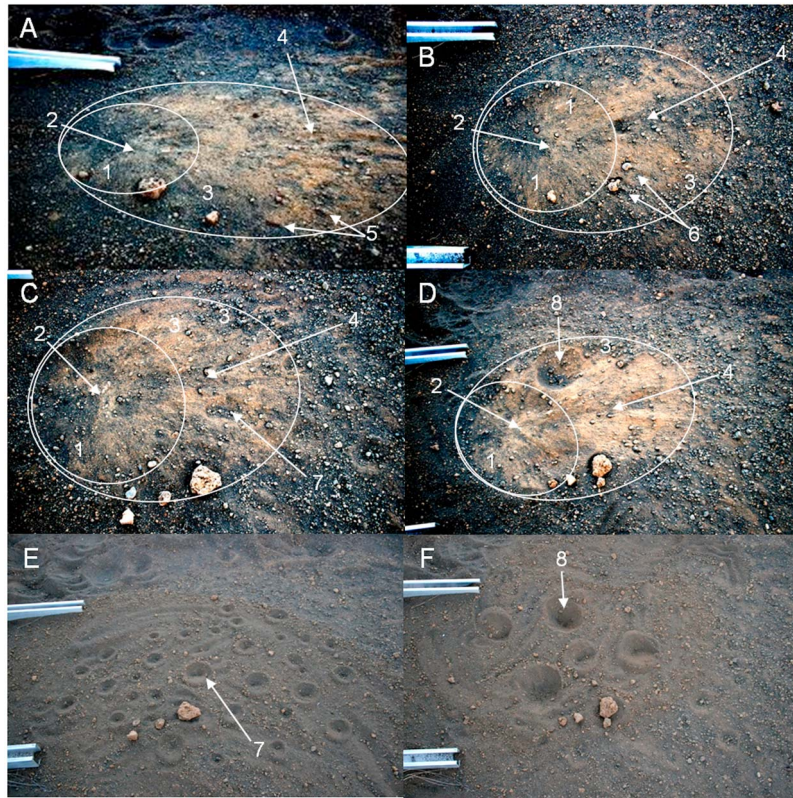


**Figure 18.** Residual brightening of eroded surface (contrast enhanced). Direction of gas flow was left to right. (a–d) Test cases 1 through 4, respectively (contrast enhanced); (e and f) test cases 3 and 4 prior to thruster firing, for comparison. Features are (1) circular crater, (2) central bulge, (3) shallow pan, (4) axial flute, (5) examples of erosional remnants, (6) examples of flutes trailing obstacle scour, (7) example of partially survived crater, and (8) crater that survived intact except for its raised rim.

air and dissipated. While this is analogous to the clearing stage of the Apollo landings, the transport mechanisms of dust appear to be unrelated. In the Mauna Kea field tests, no dust was lifted from the surface after jet cutoff. The tephra would not be pressurized significantly by the subsonic end of the jet in an ambient atmosphere, so there should have been no gas diffusion from the subsurface to lift dust. There may have been electrostatic charging of the soil by the plume, but apparently in Earth’s gravity it was insufficient to lift the dust.

[29] As shown in Figure 18, the terrain at and around the impingement point was found to have been left visibly brighter with a yellowish appearance relative to the darker gray of the bulk tephra. This might be analogous to the brightening around the Apollo landing sites. The gravel, which had been transported as bed load, was concentrated in a wide band just beyond the brightened zone. The brightened zone was identical to the region in which erosion occurred, as indicated by the lowering of the surface. This zone was roughly elliptical with a downrange length of about 60 cm and a width of about 30 cm. The upstream end that included the impingement point was deeper, consisting of a roughly circular crater that was about 3 cm deep. The remainder of the ellipse (downstream from the impingement point) was a flat, shallower pan of about 6 mm depth. An “axial” flute extended along the direction of the jet through

the elliptical pan. The total eroded volume was on the order of 1.6 L, indicating an erosion rate of about  $800 \text{ cm}^3/\text{s}$  or about 1 kg/s during the two second thruster firing. There were no ripples or dunes in the eroded bed, indicating that soil was removed and not significantly redeposited within that region. There were however some radial bed forms: several flute-like structures (negative relief features: grooves parallel to the flow where erosion had been greater than the surrounding surface) and many erosional remnants (positive relief features) each headed by an embedded piece of gravel. There were also numerous examples of obstacle scour (scour pools surrounding embedded gravel or cobbles). These corresponded to locations where dust tails had occurred, as discussed above. The flutes were usually a radial elongation of obstacle scour. Thus, both flutes and erosional remnants began at embedded gravel or cobbles. Apparently an obstacle maintained an erosional remnant until obstacle scour was initiated. The obstacle scour removed the soil around the object and also the erosional remnant behind the object, leaving a flute in its place. This liberated the obstacle, which rolled out of its scour pool and blew away. The large quantity of soil removed from around and behind the obstacle during this process released its cargo of dust, producing the bright dust tail.

[30] We found that the brightening of the soil in the eroded zone was a thin veneer of dust that would immedi-

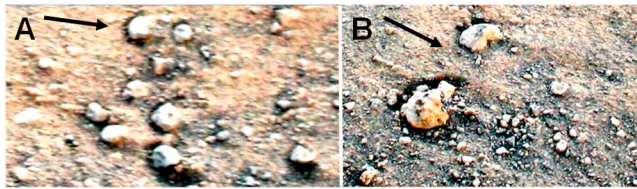


**Figure 19.** Variations of brightening on short length scales is negatively correlated to erosion (contrast enhanced). Arrows show approximate direction of gas flow. (a) Erosional remnants behind particles of gravel. (b) Two examples of obstacle scour.

ately go into suspension and fly away when disturbed by kicking, leaving the ground the original gray color. If we did not mechanically disturb this bright dust layer, it would persist as long as we continued to observe it (i.e., it would not go into suspension and leave through nominal wind at the test site). This was counterintuitive, because the slightest mechanical disturbance removed the dust and so it seemed that the rocket exhaust and the erosion of the bulk soil from beneath it should have been able to remove it. To explain this, we have considered several possibilities. First, perhaps the dust became concentrated on the surface after the thruster was shut off. But suspended dust would stay suspended and drift far away from the test site, not falling back to coat the surface in the impingement zone. Second, perhaps a portion of the suspended dust was electrostatically attracted back to the impingement zone after the thruster cut off. The hot plume gas of a rocket is generally charged as it exits the nozzle [Sabaroff, 1965], and may deposit a net charge onto the surface, which could then attract the dust back after the high velocity gas flow ends. However, this does not explain why the liberated dust was not also charged by the plume gas so that like charges would have repelled, or how it was so effective at attracting such a large quantity of dust out of the very dilute suspension. It seems more likely that the dust was concentrated at the surface during the erosion process itself, not just by mechanisms operating after the thruster had cut off. This leaves two more possibilities. One is that larger particles are preferentially removed in the erosion process, leaving the dust-sized particles to concentrate on the surfaces wherever erosion was taking place. This is difficult to imagine, though, because removing the larger particles out of the bulk would seem to disturb and release all the neighboring dust particles into the boundary layer at same time, and that is in fact what generally occurred in these experiments as ridges were blown away in bulk and during obstacle scour: erosion of bulk soil released the dust from that soil into bright streaks, dust tails, and suspension.

[31] The other remaining possibility was suggested by a close examination of the surface. The brightening was nonhomogenous over several length scales and negatively correlated to the amount of erosion. Figure 18 shows that the circular crater immediately around the impingement point in cases 1 through 4 was generally darker than the shallow pan, in which less erosion occurred. Each of these circular craters had a (poorly defined) central bulge where erosion was slower due to stagnation of the gas at the impingement

point, and these central bulges were generally brighter than the surrounding crater. The axial flute where erosion was faster was darker than the pan through which it had cut. On smaller length scales, Figure 19a shows several partially embedded pieces of gravel with erosional remnants in their wake. These remnants, where erosion was slower or where deposition was occurring, were brighter than the surrounding soil. Furthermore the surface between the largest gravel, where gas flow would have been least smooth and therefore erosion most rapid, was darker than some other nearby surfaces. Figure 19b shows two pieces of gravel in scour pools that were elongated downstream. A raised ridge like an unusually thin erosional remnant also stood in each one's wake in the midst of the elongated scour pools. Apparently these objects were undergoing obstacle scour, which was converting the erosional remnants into flutes, at the time thruster cut off so that the intermediate state survived. The scour pools where more erosion occurred are seen to be darker, whereas the thin erosional remnants and the surrounding soil are generally brighter. Variations of surface brightness can also be seen on smaller length scales around even smaller objects in each frame. Altogether, it appears as though dust was being constantly redeposited very close to all eroding surfaces so that it accumulated wherever erosion was slower or not occurring. Surfaces undergoing dust deposition would become more aerodynamically smoothed by this coating of dust, resulting in smoother gas flow and lower shear stress over those surfaces, thus further slowing or stopping erosion in those areas. Thus, dust deposition would produce positive self-reinforcement over small length scales. It appears the best explanation for the brightening in the erosion zone is that erosion of a poorly sorted regolith is a very nonhomogenous process so that while soil is being removed in one location it will not be occurring very close by, and so a significant fraction of the released dust is immediately redeposited onto adjacent locations within the erosion zone.

[32] It is not necessarily unreasonable that dust would be redeposited over very short distances from where it was recently eroded/released, because simulations show that dust-sized particles have the least aerodynamic lift in the velocity gradient of the boundary layer and thus would remain closest to the surface [Lane *et al.*, 2008, 2010]. It has long been known that it is more difficult for a gas flow to lift dust-sized particles  $<10 \mu\text{m}$  or so from the surface [Iversen and White, 1982]. These results suggest that it is also more difficult for the gas flow to lift them out of the viscous sublayer and thus keep them from immediately redepositing.

### 3.4. Test Results for Varied Surfaces (Cases 3–9)

[33] Several of the phenomena described above have been noted during the Apollo landing videos, although on a much different size scale. We decided in case 3 to enhance the similarity by putting a number of small-scale “craters” in the impingement area to see if the dust-blowing phenomena associated with lunar impact craters would be observed in these tests. In the Apollo landings the craters in the field of view were in the meter size range. The craters in our test ranged in size from 1 to 4 cm diameter and always with a depth about half the diameter, similar to the lunar crater depth/diameter ratio. During the first few milliseconds of

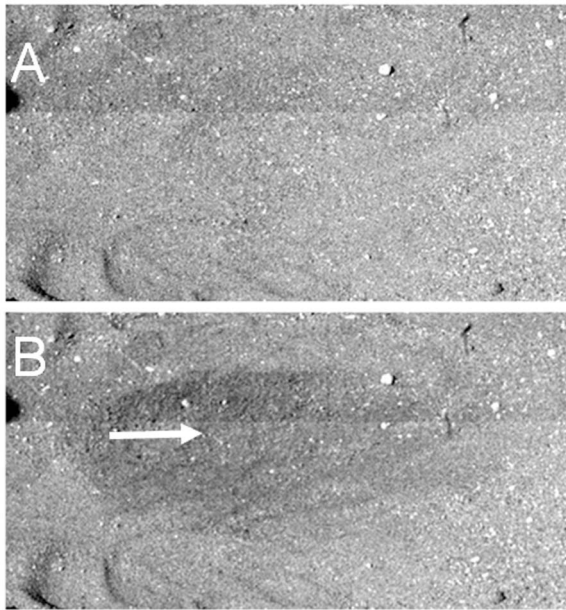


**Figure 20.** Case 7 (a) before ignition and (b) during the splash stage. The dust ring is absent. Arrow shows the direction of gas flow from the impingement point (reverse perspective compared to Figures 15).

thrusting, in the splash stage, the plume impingement lifted dust at an enhanced rate around the rims of each crater as indicated by brightening that occurred there, shown in Figure 15c. Unfortunately, the craters did not survive more than a few milliseconds and were rapidly wiped away either by filling in or by removal of surrounding soil or both. Therefore in case 4 the craters were made fewer and larger, between 4 and 8 cm in diameter with the same depth/diameter ratio approximately 0.5 as before. This time the largest craters persisted for the duration of the 2 s firing. As before, complete dust rings formed around the crater rims in the splash stage as shown in Figure 15d. The rims were then rapidly removed, but the craters persisted and enhanced erosion as indicated by dust streaks continued from the leading and trailing (windward and leeward) edges of the craters throughout the firing.

[34] In case 5 with vibrationally compacted tephra the dust liberation rate was reduced somewhat relative to the unmodified tephra, as seen by the reduced opacity of the dust ring in Figure 15e. The bulk soil erosion appeared also to have been reduced somewhat as seen posttest by a reduced net lowering of the surface in the impingement zone. There were no other qualitative differences between case 5 and cases 1 through 4. In case 6 with vibrated and tamped soil there was perhaps some further modest reduction in erosion rate and dust liberation rate as seen in Figure 15f, but it was less than an order of magnitude different.

[35] In cases 7 through 9 with the graded soil there was no visible dust liberation, which would normally appear as brightly illuminated streaks or clouds, although bulk soil was still removed. The dark spot in the splash stage shown in Figure 20 was due to increased surface texture and thus shadowing, indicating where the bulk soil was being

removed. The absence of liberated dust was probably due to remnant moisture in the soil that adhered the dust-sized particles onto the larger ones as they were eroding. While working with the graded soil, we realized that despite the arid desert character of the test site the soil had moisture content around 10% below about 10 cm, which had a dominant effect on the soil strength at that depth. We also noticed that the soil exposed by grading would dry thoroughly in situ in less than 24 h to near 0% moisture content in the upper several centimeters. This surface had been excavated to about 20 cm depth in the grading process and left to dry overnight. However, in the vicinity of the thruster test rig where there was a lot of personnel traffic, a lid was placed (without our knowledge until posttesting) over the soil overnight to protect it from footfall disturbance. This most likely retarded the drying process. Future work will require more carefully controlled moisture content. Dust-sized particles would be most affected by the remnant moisture. A second thruster firing (case 8) confirmed the low erosion rate and lack of dust liberation observed in case 7. As a check, the soil was cultivated from its compact natural state by raking fingers through it and then leveling lightly by hand, after which it was subjected to an additional firing (case 9) in the same late afternoon lighting conditions and with the same camera settings. An increased erosion rate was confirmed due to cultivation, although there was still a remarkable absence of brightly illuminated, liberated dust, implying a cohesive effect of residual moisture.

[36] The moisture content was serendipitous as it caused the erosion in both cases 7 and 8 to occur in thin layers, or laminae, as shown in Figure 21. The thickness of these laminae was on the order of 1 mm. Examining Figure 21 carefully, it can be seen that they alternate between fine and coarse particles. Coarse particles are less cohesive and more easily removed by the plume than are the fines in the presence of remnant moisture. Close to the impingement point it appeared that the intervening coarse layers were completely removed. Further away from the impingement



**Figure 21.** Lamination in soil exposed during case 7 (contrast enhanced). F, fine layers; C, coarse layers; C\*, presumed location of coarse layers completely removed by plume; A, unheaded erosional remnants. Note brightness in eroded region, in this case due to removal of coarse particles.

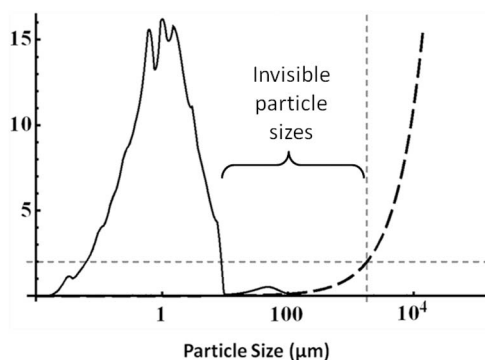


**Figure 22.** Visibility of different particle sizes in recorded videos. Solid curve indicates surface area of blowing lunar soil per micron particle size ( $\text{cm}^2/\mu\text{m}$ ). (This is scaled for an arbitrary quantity of soil.) A similar analysis has not been performed for test site tephra, but the overall mass fraction below  $10 \mu\text{m}$  is comparable to lunar soil, so the visibility of tephra dust is expected to be similar. Heavy dashed curve indicates camera pixels per individual particle at the test site. Light dashed lines indicate guides to the eye at  $1800 \mu\text{m}$  and 2 pixels.

point, where the shear stress was less, the coarse layers partially survived. Presumably these tephra laminations were formed by seasonal deposition of reworked tephra, perhaps through Aeolian transport. Transport of thin layers of granular material is known to produce size segregation with the coarser particles rising to the top. Thus, each lamina (consisting of coarse particles on top of fines) may represent the deposition of one year. The plume acted as a sensitive method to peel apart the individual laminae, which otherwise would have been difficult to identify. When the soil was disturbed and relevelled for case 9, the plume formed a smooth-bottomed crater with no laminae.

## 4. Discussion

### 4.1. Invisibility of Blowing Bulk Soil

[37] While interpreting the video imagery from the field tests and from the Apollo landings we noticed that mid-sized particles cannot be seen moving, although both clouds of dust and pieces of gravel can be. We calculated the contribution of each particle size range to the overall optical density of the blowing material using the particle size distribution of lunar soil. This was based on the submicron particle size distribution measured by *Park et al.* [2008] and used the complex index of refraction of the soil and the equations of Mie scattering [*Gebhart, 2001*]. Details are given by *Metzger et al.* [2010b]. The result of this calculation is shown in Figure 22. The surface area (per micron of particle size) contributed by the  $10 \mu\text{m}$  size fraction is 1.5 orders of magnitude greater than the contribution from the  $60 \mu\text{m}$  size fraction, and it is 5.5 orders of magnitude greater than the contribution from the  $1000 \mu\text{m}$  size fraction. The dynamic range of brightness values of a digitally recorded (or digitally converted) video is limited by the number of bits in the data word representing each pixel. Because the brightness of the light reflected off the larger particle sizes is so many order of magnitude less than the

brightness reflected off of the  $<10 \mu\text{m}$  sized particles, it represents less than 1 bit level of brightness, and thus cannot be represented in the digital video. Thus, blowing masses of particles  $>10 \mu\text{m}$  will be invisible or at best difficult to see when the camera is set up to record the bright, blowing dust clouds. This will be generally true for any dusty soil where the optical density, and thus the dynamic range of the brightness values, is dominated by the dust fraction. We do not have submicron particle size distribution data for the soil at Mauna Kea as we do for lunar soil, but the dust fraction  $<10 \mu\text{m}$  is comparable to that of the lunar soil (compare Figure 12). Whereas the dust is observed as a cloud (and not as individual particles), the gravel-sized particles and larger can be seen individually. This is true whenever the particle image covers more than 2 pixels of the camera so that the bright and dark sides of the particle create a visible contrast in the image. In the field test videos the pixels cover about  $900 \mu\text{m}$  at the distance to the soil's surface, and thus individual particles that are  $>1800 \mu\text{m}$  can be identified. In the Apollo landings film cameras were used, but the limitations are analogous to those of digital cameras. Rocks visible in the Apollo landing videos when the LM was about 2.3 m above the lunar surface have been photogrammetrically measured by *Immer et al.* [2008] and based on the same images we crudely estimate that gravel as small as 1 cm can be distinguished against the background when the lander is at the same altitude. Therefore, all the blowing material in the size range of approximately  $10 \mu\text{m}$  to 1.8 mm will be invisible in the field test videos, and the size range of approximately  $10 \mu\text{m}$  to 1 cm will be invisible in the Apollo landing videos. In each case, the invisible range includes about 90% of the mass of the soil. Its motion cannot be seen but instead must be inferred by the visible release of dust representing only 10% of the mass, the release of gravel or rocks, and the cumulative changes in terrain shape.

[38] Although unseen in the field test videos, the sand-sized particles must have been moving because the removal of bulk soil would be needed to ensure a continuous supply of new dust. It is not known how the sand-sized particles moved, whether through rolling, saltation, or sustained aerodynamic flight in the high velocity gas. Likewise in the Apollo landing videos, the total quantity of blown dust as measured by its optical density implies that several tons of soil had been blown to release that much dust, as discussed below. Simulations of lunar plumes show that the sand- and gravel-sized particles should be lifted aerodynamically and blown away without saltation [*Lane et al., 2010*].

### 4.2. Erosion Rate Versus Soil Density

[39] In the field tests the plume removed the loose tephra in cases 1 through 4 at a higher rate than it did the more densely packed vibrated and tamped tephra in cases 5 and 6 as indicated by the optical density difference of the liberated dust. The top layer of the lunar regolith is uncompacted material, kept loose by micrometeorite impact "gardening" [*Lindsay, 1976*]. The deeper layers are believed to have been densified through the vibrations and shock waves of these same micrometeorite impacts [*Carrier et al., 1973; Houston et al., 1974*]. The "swept clean" appearance after Apollo landings indicates that the loose, uppermost part of the soil had been blown away from the immediate vicinity of the LM, leaving a generally hard-packed surface with partially



**Figure 23.** Rock under Apollo 12 engine bell. (Detail from NASA photograph AS12-48-7034HR.)

embedded cobbles and gravel. By analogy with the field tests, the erosion rate must have slowed but not stopped after the loose top layer of material was depleted. A trajectory with a significant horizontal velocity component would fly over new, loose surface material, keeping the erosion rate high, whereas a more vertical descent trajectory would minimize the erosion rate and the total quantity of blown soil. This contradicts a conjecture by *Scott* [1975] that the more vertical trajectory of the Apollo 12 landing may have resulted in an increased erosion rate and reduction of visibility relative to Apollo 11, which had a more horizontal trajectory. It seems more likely the vertical trajectory should have slightly reduced the erosion rate, and the reduced visibility in Apollo 12 is better attributed to the lower sun angle in that mission. Also, the soil varied significantly between the different landing sites in regard to its maturity, compaction, and other properties, and this would have a significant effect on erosion rate. For example, in Apollo 15, which had one of the worst cases of visibility due to high dust density during landing, *Scott* and *Irwin* commented that there was about 15 cm (6 in) depth of very soft soil, like powdery snow, close to the LM [*NASA Manned Space Center*, 1971c]. A more detailed analysis of this dependency would require not only the top layer of soil be analyzed at each landing site, but each underlying layer to the depth that the plume eroded during landing.

#### 4.3. Effects of Cohesion on the Surface

[40] Cohesion was seen to play a role in lunar soil erosion because of the formation of unheaded erosional remnants and the hummocky texture. The soil at the Mauna Kea test site was noncohesive when dry, unlike the dry yet cohesive lunar soil, which is much finer, is at lower gravity where cohesion is relatively more important, and has agglutinate particles with interlocking shapes. However, unheaded positive relief features similar to those in lunar landings were seen in the field test when (and only when) the soil had remnant moisture and thus cohesion, as in Figure 21 region A, confirming that these features are an indicator of cohesion. The cohesive effects on lunar soil erosion are important to quantify so that physics simulation codes can accurately predict the ejection of material.

[41] To construct a landing zone near a lunar outpost, palliatives have been considered as an additive to the soil to increase cohesion and help to hold down the soil. This is the practice at terrestrial desert air strips. However, the field tests indicate that modest increases of cohesion will not stop erosion but will only slow it. Hardware surrounding the landing zone will still be subjected to the high velocity spray of ejected soil and consequent damage [*Clegg et al.*, 2008; *Immer et al.*, 2011]. On the other hand, modest increases of cohesion will cause the dust fraction to cling to the larger sand-sized particles and to each other, thus vastly reducing the optical density of the blowing material as indicated by Figure 22. This may be beneficial to increase visibility during landing, but in general is an inadequate solution to the plume problems. Experiments are still needed with heavier applications of palliatives to measure their effectiveness, and trade studies should evaluate the mass of palliative that must be brought from Earth.

#### 4.4. Dust Tails and the Blowing of Rocks

[42] In the Apollo program it was commonly believed that the LM exhaust was incapable of blowing anything larger than gravel, and thus incapable of inflicting large momentum impacts to any hardware positioned on the lunar surface in that vicinity. This belief was based on the analysis of *Roberts* [1963, p. 23], which in the era before digital computing was unable to account for the details of the lunar boundary layer and thus unable to accurately calculate the aerodynamic forces on particles. *Roberts*' equations predict that particles only up to 3 cm could be lifted by a lander with 4500 N (10,000 lb. feet) thrust at 30 cm (1 foot) altitude. The LM with nearly empty descent fuel tanks would use much less thrust at that altitude. The belief that "rocks do not blow" was supported by the discovery that some rocks did indeed remain beneath the LMs very close to the engine nozzle after landing. *P. Conrad* stated in the Apollo 12 technical debrief [*NASA Manned Space Center*, 1969d]:

Now the one comment I made in flight was that there was a rock about 3 by 4 by 2 inches [ $8 \times 10 \times 5$  cm] lying right under the engine bell. It hadn't been blown away. I can't figure out how it was lying right out at the skirt edge. We took a photograph of it. I don't know whether it will show or not, but it didn't get blown away. I was quite surprised after seeing all that dust and stuff flying on landing that it did not blow a rock that size away.

[43] However, finding rocks beneath the LM does not prove that the plume cannot blow them away. It could be that the rocks were freshly exhumed when engine cutoff occurred and so they did not have time to blow away. More importantly, the gas velocity is at a minimum under and near the engine bell and that is the place where the plume is least able to blow rocks. Also, it is not clear that there were actually any loose rocks beneath the LM. The rock reported beneath the LM by the Apollo 12 crew and shown in Figure 23 appears, upon close examination in every available photograph, to have been embedded in the soil and not actually loose. Likewise the rock seen in Apollo 14 was embedded as shown in Figure 7 (inset). (Some loose material in that photograph was generated by footpad impact, but the rest of the surface was swept clean.)

[44] More recently, *Phillips et al.* [1988] claimed that particles larger than 5 mm could not be blown. The details

of their analysis were not provided, but they stated that it was calculated from the stagnation pressure of the plume gas beneath the particles. The plume flow solution they cited [Alred, 1983] as the basis of their calculation was for a thruster in free space and not impinging on a surface, so the analysis neglected the radial flow away from the stagnation region and the boundary layer that develops over the lunar surface. Therefore it cannot be correct.

[45] On the other hand, *Immer et al.* [2008] interpreted two objects in the Apollo 14 landing video to be rocks blown away by the plume and photogrammetrically measured them to be 11 to 15 cm in diameter. After being exhumed, they appeared to become elongated before leaving the field of view. *Immer et al.* [2008] conjectured that these elongations were dust tails forming behind the rocks as they were exhumed. The Mauna Kea field tests affirm that interpretation. An alternate hypothesis is that these two objects were not really rocks, but were instead friable clods of loosely cemented soil, and that their elongation was evidence that they were falling apart in the plume and blowing away as a stream of small particles, not moving as solid objects the size of rocks.

[46] This is a serious concern for launching and landing on the Moon in the presence of a lunar outpost or scientific instruments, which could be irreparably damaged by a large rock strike. Therefore it is important to confirm that rocks do blow and to quantify the damage they could cause so that premission planning can find ways to minimize these risks. Recent analysis using modern gas flow codes of LM plumes impinging on the lunar surface has shown that the LM plume should indeed have been capable of lofting particles at least as large as 1 cm [Lane et al., 2008, 2010]. We have now extended these results using the same software. This method predicts that 1 cm gravel should be ejected with velocities on the order of 30 m/s, whereas 10 cm rocks should be ejected with velocities on the order of 9 m/s. This analysis takes into account the full plume flow field including the boundary layer, with the lift and drag forces on the rocks accounting for the rarefaction, compressibility and Reynolds number. However, parts of the physics are still neglected such as momentum transfer through collisions of different sized particles and a realistically varying lunar topography, so empirical confirmation is needed.

[47] We have performed a careful frame-by-frame examination of the Apollo descent videos and have found many cases of rocks blowing, even while the LM was quite high. They were difficult to identify because random noise in the videos also has the appearance of rocks, and because in most instances the rocks were already airborne when they first appeared in the field of view and thus were more difficult to distinguish from the random noise. They were confirmed to be rocks by their coherent shadowing (which the random noise lacks), and because in some cases they could be tracked radially away from the LM through multiple frames of the video. These rocks were about 4 to 10 cm in diameter. There was no apparent elongation of these rocks in the direction of travel relative to the transverse direction, so shutter speed was not significantly affecting the image of the rocks. They were traveling about 11 to 30 m/s when tracked for multiple frames (with smaller rocks traveling faster), so the simulations are in excellent agreement.

[48] We found, in addition to the confirmed airborne rocks, many cases of dust tails. We have interpreted these, on the basis of the field tests, as the indicator that obstacle scour has begun around an embedded cobble. The termination of the dust tail is the indicator that the cobble has been ejected from the soil. The duration of dust tails in the Apollo landing videos (~100 ms) agrees well with the field tests, wherein a large piece of gravel forms a dust tail, begins moving, and loses its tail within 100 ms, whereas a larger rock could take 200 ms. In the Apollo landings the dust tails persist about 100 ms even with the larger thrust, implying they are larger rocks. In these cases the rocks themselves were not visible because they were beneath the dense dust sheet and relatively far from the camera. In the still photographs of the terrain under the Apollo LMs, there were few cases of embedded objects with attached erosional remnants because the plume has rapidly blown most of them away in this fashion.

#### 4.5. Bed Load Transport

[49] In the Apollo landing videos we have not identified any bed load beneath the dust sheet similar to what occurred in the field tests. This may be due, in part, to the dust sheet obscuring the view. We have instead found rocks that blew and rarely skipped with saltation lengths longer than the field of view. This can be explained by the lower lunar gravity and the larger thrust of the LM plume compared to the field test. Presumably a bed load of gravel- and cobble-sized objects would have existed closer to the stagnation region under the nozzle where dynamic pressure of the plume is less. Supporting evidence for bed load transport is the series of skip marks in Figure 10, which must have occurred late in the descent since they were superimposed on top of the unheaded erosional remnants. Thrust may have been reduced at that stage of landing; if the rock at the end of these marks was their cause, then they occurred as the engine was shutting off. Beyond the radius of a meter or two only the largest rocks should have continued as bed load, but they are not abundant. Nonetheless, it is possible that in each Apollo landing some larger rocks were excavated by the plume and displaced exclusively through bed load transport, obscuring their geological context while leaving them in the vicinity of the LM where they could be found loose on the surface. This should be kept in mind for returned rock samples as well as for future lander missions. This mode of transport under the LM is important to quantify in order to accurately predict the net soil erosion, since it fed material into the annulus where aerodynamic lifting took place and because the mechanical interaction of this bed load with the surface helped to loosen and eject other material.

#### 4.6. Soil Erosion in Discrete Layers

[50] Perhaps the most interesting finding is the erosion of soil in discrete layers, both in the Apollo landings and the field tests. In the latter, erosion in layers only occurred in cases 7 and 8 when the thruster fired on undisturbed soil (so it could have natural laminae) and when there was significant moisture content causing cohesion in the fines. In the lunar landings, the lunar soil always has natural layering and is known to have significant cohesion, and indeed the ero-

sion by discrete layers was confirmed on most missions where numerous photographs were taken beneath the LM.

[51] One question is whether the plume was eroding to the horizons of natural soil layers, or whether the thickness of the removed layer was determined purely by gas flow/erosion dynamics and had nothing to do with geological layers. Experience shows that gas flow/erosion dynamics do not create distinct layers with straight-walled contacts of consistent size. There is no known mechanism by which it could. Positive evidence that the layers were natural laminae in the field tests are that the thickness of layers along the contacts was consistent; and the layers alternated between coarse and fine particle sizes in the crater. This provides a plausible mechanical means by which the plume could separate the laminae and create sharp terraces. In case 9 where the only difference in the soil conditions relative to cases 7 and 8 was that the natural laminae were destroyed by mixing, then no layering appeared in the crater.

[52] The field tests suggest that the terracing in the lunar landings was likewise due to natural geological strata. The difference in mechanical competence that allowed one layer to be stripped away while leaving the next lower layer intact may have been due to an abrupt change in compaction, particle sizing, or the agglutinate abundance. Compacted soil is more cohesive because it has a larger number of grain-to-grain contacts (each with cohesive energy) per unit volume of soil. Likewise, soil with a greater abundance of fines has more grain-to-grain contacts per unit volume and is more cohesive. Agglutinates have interlocking shapes, which produce effective cohesion in the soil. In every observed case of stripped away upper layers identified here, the horizon (boundary) between the upper and next lower layer was very well defined, indicating an abrupt change in the soil compaction, particle sizing or agglutinates, not a gradual change. Thus, if the mechanical difference is attributable to compaction, this indicates a refinement to the model presented by [Carrier *et al.*, 1991, Figure 9.16], which shows a smoothly increasing compaction with depth. The stratigraphic soil layers correspond to the particular lunar impact events that created them. Thus they each have distinct ages and overlying layers may be abruptly less compacted due to their younger age and less time exposed to micrometeorite tamping [Carrier *et al.*, 1973; Houston *et al.*, 1974]. If it is an abrupt change in the particle size distribution or agglutinate fraction that makes the overlying layer distinctly more erodible than the underlying layer, this too may be explained by the age of the strata, since mature soil tends to be finer with more agglutinates and the overlying soil may be less mature and thus more coarse and with fewer agglutinates. Furthermore, because gardening causes maturation only in the top few millimeters of a stratigraphic layer [Lindsay, 1976], the uppermost “skin” of each layer may be more resistant to the plume than the rest of the layer. Thus, as long as the skin of the layer did not fail, the weaker soil beneath it was protected. But once the skin was compromised, the layer may have begun failing contiguously along the contact.

[53] In the field tests, the deepest erosion and greatest number of removed layers was at the impingement point, because the gas was turbulent and had the highest turbulent kinetic energy at that point, despite it being the symmetry point in the so-called “stagnation” region [Haehnel and

Dade, 2008]. Therefore, the eroded layers were stepping uphill away from that point. In contrast to this, in the Apollo landings the maximum removal of soil is never directly beneath the nozzle but instead appears about a meter or more away from the impingement point [NASA Manned Space Center, 1971a]. Thus, the eroded layers were stepping downhill away from the nozzle. This is understandable because the core of the plume was inviscid and nonturbulent, and beneath the shock near the nozzle it was stagnant, so it should have been nonturbulent beneath the LM. Thus the highest turbulent kinetic energy as well as the highest shear stress would have been in an annulus, and erosion rate would be at a maximum in an annular region corresponding to where the most soil layers were removed. Indeed, in the Apollo 11 landing in particular, shown in Figure 9, the removal of the upper layer appears to have been in a roughly annular region around the nozzle with a fairly well-defined radius. A similar partial annulus can be identified toward the rear of the LM in the Apollo 14 imagery (e.g., on the left side of Figure 7).

[54] Because the uppermost layer was swept clean indicating that the loose material had been entirely removed from the surface, it is likely that entire epiregolith [Mendell and Noble, 2010] and perhaps one or more geological strata had been removed. The annular stripping effect at the time of engine shutdown was therefore exposing whatever layer was the next one down the geological column. The number of removed strata may be estimated by calculating the total mass of removed soil.

#### 4.7. Total Mass of Removed Soil

[55] The mass of soil ejected during a lunar landing depended upon the thrust (and hence the trajectory profile) of the LM and the conditions of the soil at the landing site. Several methods have been used to estimate the total quantity of soil blown during the Apollo lunar landings. None of these methods is accurate enough to account for the differences in the six landings. Their goal is to estimate the order of magnitude of blown soil roughly representative of all six landings.

[56] Mason and Nordmeyer [1969] performed small-scale experiments of a thruster in a vacuum chamber and compared the crater size to photographs of the surface under the Surveyor V lander to derive an erosion rate equation. This equation was applied by Mason [1970] to the Apollo 11 landing to estimate that only 36 to 57 L of soil were removed, which equates to about 0.11 to 0.18 MT. Scott [1975] performed calculations based on the total surface scouring of the Surveyor III spacecraft by the soil ejected from the nearby Apollo 12 landing, and while some portions of the method were not reported, it seems his method predicts between 1460 and 2080 L of soil were ejected, amounting to about 4.5 to 6.4 MT. (This is based on the assumption that he used cylindrical geometry for the eroded region of soil, but if not, the order of magnitude of his results is nonetheless the same as reported here.) Metzger *et al.* [2008] modified Roberts' equations [Roberts, 1963] by integrating over the lunar soil particle size distribution and used the Apollo 12 trajectory to estimate that 787 L, or 2.4 MT, of soil were ejected. Using the Apollo landing videos, Immer *et al.* [2008] measured the optical density of the blowing dust to obtain several estimates of its mass

density. That method accounted for the unknown camera settings by comparing image brightness in dark and illuminated regions both with and without blowing dust present. Metzger *et al.* [2010b] used that method along with the equations of Mie scattering and the lunar particle size distribution to estimate the blowing flux of soil at several points in space and time during some of the Apollo landings. Immer *et al.* [2011] used that result to crudely estimate the time-integrated flux of ejected soil at  $m = 0.02 \text{ g/cm}^2$  at a distance of  $R = 155 \text{ m}$  from the LM. This assumed the flux was uniformly distributed from the ground up to  $\theta = 2.3$  degrees, based on the measured angle of the dust sheet. Assuming it was also uniform in azimuth around the lander, the total mass of ejected soil can be estimated at  $M = 2 \pi m R^2 \tan \theta = 1.2 \text{ MT}$ .

[57] This last method assumes the dust and bulk soil are proportioned as per the particle size distribution. However, the field tests indicate that the relationship between dust liberation and bulk soil erosion rate is not a simple relationship. Cohesion in cases 7–9 caused the dust to cling to the soil and thus the optical density of the eroding soil underpredicted the bulk erosion rate. In the field tests this was probably due to the residual moisture, but in lunar landings the dust liberation may have been affected by other natural forces such as Van der Waals or electrostatics. However, because the plume was ionized [Sabaroff, 1965], it is likely that electrostatic agglomeration was minimized. Also, during the terrain modification stage, the ejected soil is sometimes so dense that it becomes opaque, and then it is impossible to quantify optically. Thus, the soil erosion rates calculated by optical density could be an underestimate.

[58] These estimates based on different methods disagree by almost two orders of magnitude. The photographs under the LM roughly indicate the depth of erosion and may be used to evaluate if any of these estimates is reasonable. The soil was swept clean to a smooth-appearing layer in the soil, which implies that at least the uppermost, loose deposit of soil was completely removed. Figure 9 suggests at least one additional layer of soil was stripped away in an annular region. The small steps in region B of that photograph indicate that it is not just one layer being eroded at that radius. The soil contact in Figure 10 implies that soil layers are still stepping downhill moving away from the nozzle as far outward as the footpads. Plume simulations indicate that the majority of soil erosion should have taken place within a radius of about 3.5 m because shear stress of the gas becomes small beyond that distance when the lander is at low altitude. Somewhere between the footpads and 5 m the soil layers must begin stepping back up. We adopt this simple model: one entire “layer” is removed over a 3.5 m radius; a second layer is removed between the 1 and 2.5 m radiuses; a third layer is removed between 1 and 2 m. Lindsay [1976] reported that the distribution of lunar strata thicknesses is bimodal, with the dominant mode at 1.0 to 1.5 cm and a minor mode at 4.5 to 5.0 cm. The mean appears to be on the order of about 2 cm. Lindsay reports that the mixing zone from micrometeoroid impacts is about one millimeter, with the overturning of soil occurring at a much reduced rate below that, so the strata typically survive for long times. Using a 2 cm thickness for the “layers,” the depth of erosion in the center of the annulus is 6 cm. Using an estimate of bulk density of about  $1.4 \text{ g/cm}^3$  for the loose, upper layer of the soil [Carrier *et al.*, 1991], the volume of this model re-

presents 1.80 MT of soil blown away by the plume. This is in agreement with the order of magnitude of the erosion estimates based on optical density and Roberts’ equations. It is an order of magnitude higher than the estimate of Mason, and a factor of 2 to 4 lower than the estimate of Scott.

[59] There are not many loose cobbles or gravel under the LMs (except for those mechanically liberated by footpads or contact probes), but this is consistent with the observation that the plume ejects them via bed load transport out to the radius where they are lifted and blown. Thus, large quantities of soil could have been blown away without leaving a gravel bed behind. Also, rocks in the field of view out the windows were exposed then liberated and ejected very quickly in the videos, and this implies that the surface around those rocks was being lowered at a high rate, corroborating the other arguments for a high erosion rate. Superimposed upon the natural terrain variations, the lowering of the surface by 6 cm centimeters might be undetectable to the eye if it were not for the abrupt contacts formed by the removal of individual strata. In general, it is reasonable that one ton up to several tons of soil was ejected with each landing.

#### 4.8. Brightening Around Landing Site

[60] Every lunar lander mission beginning with the Surveyor program observed that the soil around the lander became darker when disturbed even slightly. This was originally interpreted as a thin, light colored veneer less than 1 mm thick lying on the surface. At first it was believed this veneer could be globally distributed, perhaps the result of solar bleaching [Cohen and Hapke, 1968], or a particle size sorting effect [Filice, 1967], or the removal of some form of patina via space weathering [Shoemaker *et al.*, 1967]. Hapke [1972] explained that it need not be a veneer; it could be explained by the lunar photometric function, a texture effect, the brightened surface being physically smooth so that disturbed soil is rougher with more shadowing at the grain-scale along its surface. When viewed at low phase angle (the sun behind the observer’s back), the difference in brightness between disturbed and undisturbed soil disappears. An example of this texture effect in the Mauna Kea field tests is shown in Figure 20, where the rougher surface indicating soil erosion appears darker. Orbital photography showed that brightening is localized around the landers [see, e.g., Hinners and El-Baz, 1972]. Thus, the physical smoothing of the surface that makes it brighter at most viewing angles was attributed to the exhaust plume of the landers [Hapke, 1972]. It was suggested by Hinners and El-Baz [1972] that the dynamic pressure of the plumes is what compacted the uppermost layer of soil. However, no analysis has been provided to demonstrate the exhaust plumes had adequate dynamic pressure over a 75 m radius. Mendell and Noble [2010] have inferred the existence of an epireolith, a layer at least  $250 \mu\text{m}$  thick but possibly much more, enriched in submicron particles in tenuous “fairy castle” arrangements. It would be responsible for the radiative properties of the lunar surface including its photometric function. This tenuous structure is stabilized perhaps by mutual electrostatic repulsion as photoelectric charging makes the dust particles positive. It could also explain the localized brightening by the plume. To brighten the surface a landing rocket need only knock down the fairy castles. Three categories of soil texture are thus noted: the undisturbed soil, smoothed by microme-

teorite tamping and covered by an epiregolith; the soil smoothed even further by the plume, presumably lacking an epiregolith; and the soil roughened mechanically by footsteps or rover wheels. Mendell and Noble suggest the epiregolith is self-repairing and rises anew with the photoionization of each lunar cycle. However, Lunar Reconnaissance Orbiter Camera (LROC) images show the landing sites still brightened some 500 lunations after Apollo, so the material that comprises the epiregolith was not simply knocked down locally by the plume. Its repair probably requires the lateral transport of new submicron dust into the zone where it was destroyed. Lunar dust transport mechanisms and rates are not well characterized, but the eventual redarkening of the landing zones may provide a way to calibrate it.

[61] There are several possible ways that a plume could change the brightness of the soil. First, heat and chemistry of the plume might affect some chemical changes of the soil's surface. This would be limited to directly beneath the lander in the stagnation region where the gas is hot and is mentioned only for completeness. Second, the static pressure of the gas could compact the soil. This, too, is an inadequate mechanism because the static pressure is vanishingly small only a meter or two away from the nozzle. Third, the dynamic pressure could knock down the epiregolith and compact it or transport it over a wider radius. This may be feasible, despite the low dynamic pressure of the plume at the radius of observed brightening, if the epiregolith particles are indeed charged and mutually repulsive. The "negative cohesion" of that repulsion could put the particles at the limit of mobility so little dynamic pressure from an exhaust plume is needed. Fourth, secondary impacts of the high velocity ejecta could impart momentum to the epiregolith and even entrain it into the dust sheet. Fifth, re-deposited dust could accumulate over some wider radius, smoothing the surface not just by knocking it down but by covering it. Sixth, the dust lifting observed during the clearing stage after engine shutoff appears to transport dust over significant heights and probably distances, although the quantity might be insignificant.

[62] The field tests suggest that dust is not easily lifted through the viscous sublayer of a gas flow and thus travels close to the surface. We suggest that the most likely explanation for the brightening is not sweeping of the dynamic pressure of the plume, but sweeping of the secondary impacts of this dust and its possible redeposition. The ejected dust sheet traveled hundreds to thousands of meters per second and easily crossed the region of observed brightening. Crew observations, simulations [Lane *et al.*, 2008, 2010] and photogrammetric measurement of the blowing dust sheet [Immer *et al.*, 2008] agree that the dust traveled in a thin sheet very close to the lunar surface. The dust-sized particles have the lowest aerodynamic lift and should have traveled closest to the lunar surface within that sheet [Lane *et al.*, 2008, 2010]. The high concentration of particles in the blowing dust layer [Metzger *et al.* 2010b] produced a low mean free path between particle collisions. Tens of meters away from the impingement point the plume gas was extremely rarefied and the dust would have traveled ballistically between collisions. At some radius the mean free path between dust collisions became large and scattering effectively ceased. Analysis of the scouring and pitting fluxes on Surveyor III by the Apollo 12 LM plume [Immer

*et al.*, 2011] indicate that it was beneath the main dust sheet (the Surveyor was located inside a crater whereas the Apollo 12 LM was located on the crater's rim at higher elevation) and was affected only by the fringes of the spray, the particles scattered out of the main sheet. At 155 m from the LM this scattering flux was sufficient to scour the Surveyor with greater than 100% surface coverage, creating scour shadows with pristine edges behind the heads of bolts. The surface of the soil near the Surveyor should likewise have received a significant flux of scattered dust. Considering this, it is surprising that the regolith brightening does not typically extend to 155 m or more. The shadows permanently etched onto Surveyor possessed no significant penumbra and pointed back toward the LM, not up toward the sheet of dust passing overhead. Thus, the radius of last scattering in the dust sheet was somewhere closer to the LM. Because Surveyor was in a crater, at lower elevation than the LM, the flux that came from that radius and impinged on it would normally have hit the soil much closer to the LM had the terrain been level. Thus, the typically 75 m radius is feasibly explained by the secondary impact of scattered dust. More research is needed, including use of the LROC imagery, to definitively explain the brightening around the landing sites and the role of each of these potential explanations, but we suggest that the secondary impact (and possible deposition) of scattered dust beneath the main sheet cannot be neglected and is probably the main contributor.

## 5. Conclusions

[63] The phenomena of poorly sorted soil erosion on Mauna Kea and on the Moon bear some important similarities, which have enabled a more extensive interpretation of the lunar case. From the comparison we draw the following conclusions.

[64] 1. The bulk of the soil eroding in the Apollo landing videos cannot be seen because of optical limitations. Only the blowing dust fraction and the motion of the larger objects like rocks are visible.

[65] 2. The majority of bed load transport was probably limited to a small radius beneath the LM and below the field of view of the windows. Beyond this only the largest rocks could continue on the surface as bed load, the remainder being lifted aerodynamically and blown away.

[66] 3. Some larger rocks could be located not far from the LM out of their original geological context, which could confuse their interpretation if collected as samples.

[67] 4. The number of smaller rocks exhumed and blown away was very large. They were ejected at high velocity during every Apollo landing and in future missions could strike and ruin instruments placed on the lunar surface or cause significant damage at a lunar outpost if they impact critical hardware.

[68] 5. Cohesion was a significant factor governing the erosion rate of soil, as witnessed by the unheaded erosional remnants and hummocky features beneath the LM, and this must be quantified through additional research so that physics-based simulation can accurately predict the erosion rates.

[69] 6. The optical density of the liberated dust may underpredict the erosion rate depending on the nature and

magnitude of cohesive forces, which could have kept the dust particles agglomerated or clinging to larger particles thus hiding their total surface area. However, the ionized plume may have reduced this effect and more research is needed to quantify and model these parts of the physics.

[70] 7. All indications are consistent so far that one ton to several tons of soil were ejected with each LM landing.

[71] 8. Soil was often stripped away in discrete steps, which may be the natural stratigraphic units in the soil.

[72] 9. The rate of soil removal ensured that the epiregolith and the top one or more stratigraphic units were completely missing beneath the LMs, and one or more additional strata were removed in an annular region (perhaps an incomplete annulus) around the base of the LM.

[73] 10. The photometric brightening over a 75 m radius around the LM's was likely caused by the secondary impact of scattered dust, ejecting the epiregolith from the brightened region. The dynamic pressure of the plume might also have blown the epiregolith directly, depending on its mobility. Some deposition may have also occurred within the brightened region.

[74] 11. Erosion can be reduced but not stopped at a lunar outpost by grading and/or compacting the soil (and we note that tamping is better than vibration to effect the compaction). Additional mitigation measures are required beside or in addition to grading and compacting.

[75] 12. Palliatives may be more effective at stopping the liberation of individual dust grains from their neighboring sand-sized particles, thus improving visibility during landing, than stopping the bulk erosion of sand and gravel-sized particles. Heavier applications might be effective at stopping the erosion entirely.

[76] While the field tests were very helpful, they also indicated how much is still unknown and how necessary it is to perform additional, more carefully conceived field tests. These results will be useful in developing physics-based simulation software that will eventually predict the erosion processes and the resulting damage to instruments and hardware on the lunar surface. The physics may also be extended to other surfaces such as asteroids, comets, other moons, and planets, where rocket exhaust will disturb the surface and affect scientific investigation

[77] **Acknowledgments.** We gratefully acknowledge Joseph W. (Bill) Studak and Brian Banker of the NASA Johnson Space Center Propulsion Branch, who built and operated the thruster in the "dust to thrust" test; Leanne Sigurdson, who performed the moisture content measurements; and Dale Boucher and his team from the Northern Centre for Advanced Concepts (NORCAT), Sudbury, Canada, who managed the 2010 field test on Mauna Kea and made the plume-soil interaction experiments possible.

## References

- Alexander, J. D., W. M. Roberds, and R. F. Scott (1966), Soil erosion by landing rockets, Contract NAS9-NAS4825 final report, Hayes Int. Corp., Birmingham, Ala.
- Alred, J. W. (1983), Flowfield description for the reaction control system of the space shuttle orbiter, paper AIAA-83-1548 presented at 18th Thermophysics Conference, Am. Inst. Aeron. and Astron., Montreal, Que., Canada.
- Bagnold, R. A. (1954), *The Physics of Blown Sand and Desert Dunes*, Dover, New York.
- Carrier, W. D., III (2003), Particle size distribution of lunar soil, *J. Geotech. Geoenviron. Eng.*, 129(10), 956–959, doi:10.1061/(ASCE)1090-0241(2003)129:10(956).
- Carrier, W. D., III, J. K. Mitchell, and A. Mahmood (1973), The relative density of lunar soil, *Geochim. Cosmochim. Acta*, 3, 2403–2411.
- Carrier, W. D., III, G. R. Olhoeft, and W. Mendell (1991), Physical properties of the lunar surface, in *Lunar Sourcebook, A User's Guide to the Moon*, edited by G. H. Heiken, D. T. Vaniman, and B. M. French, pp. 475–594, Cambridge Univ. Press, Melbourne, Australia.
- Choate, R., et al. (1964), Lunar surface mechanical properties, in *Surveyor: Program Results, NASA Spec. Publ., SP-184*, 129–169.
- Clegg, R. N., P. T. Metzger, S. Huff, and L. B. Roberson (2008), Lunar soil erosion physics for landing rockets on the Moon, paper 4122 presented at Joint Annual Meeting of the Lunar Exploration Analysis Group, the International Lunar Exploration Working Group Conference on Exploration and Utilization of the Moon and the Space Resources Roundtable, Cape Canaveral, Fla.
- Cohen, A. J., and B. W. Hapke (1968), Radiation bleaching of thin lunar surface layer, *Science*, 161(3847), 1237–1238, doi:10.1126/science.161.3847.1237.
- Collinson, J. D., and D. B. Thompson (Eds.) (1989), *Sedimentary Structure*, 2nd ed., pp. 37–47, 103–104, Unwin Hyman, London.
- Filice, A. L. (1967), Observations on the lunar surface disturbed by the footpads of Surveyor I, *J. Geophys. Res.*, 72(22), 5721–5728, doi:10.1029/JZ072i022p05721.
- Gebhart, J. (2001), Optical direct-reading techniques: Light intensity systems, in *Aerosol Measurement Principles, Techniques, and Applications*, 2nd ed., edited by P. A. Baron and K. Willeke, pp. 419–454, Wiley-Intersci., New York.
- Haehnel, R., and W. B. Dade (2008), Physics of particle entrainment under the influence of an impinging jet, paper presented at 26th Army Science Conference, U.S. Army, Orlando, Fla.
- Hapke, B. W. (1972), The lunar disturbance effect, *Moon*, 3(4), 456–460, doi:10.1007/BF00562465.
- Hinners, N.W., and F. El-Baz (1972), Surface disturbance at the Apollo 15 landing site, in *Apollo 15 Preliminary Science Report*, pp. 25–50–25–53, NASA, Washington, D. C.
- Houston, W. N., J. K. Mitchell, and W. D. Carrier III (1974), Lunar soil density and porosity, *Geochim. Cosmochim. Acta*, 3, 2361–2364.
- Immer, C. D., J. E. Lane, P. T. Metzger, and S. Clements (2008), Apollo video photogrammetry estimation of plume impingement effects, paper presented at Earth and Space 2008, 11th Biennial Aerospace Division International Conference on Engineering, Construction and Operations in Challenging Environments, Am. Soc. of Civ. Eng., Long Beach, Calif.
- Immer, C. D., P. Metzger, P. Hintze, A. Nick, and R. Horan (2011), Apollo 12 lunar module exhaust plume impingement on lunar Surveyor III, *Icarus*, 211, 1089–1102, doi:10.1016/j.icarus.2010.11.013.
- Iversen, J. D., and B. R. White (1982), Saltation threshold on Earth, Mars and Venus, *Sedimentology*, 29, 111–119, doi:10.1111/j.1365-3091.1982.tb01713.x.
- Julien, P. Y. (1998), *Erosion and Sedimentation*, pp. 93–100, Cambridge Univ. Press, Cambridge, U. K.
- Lane, J. E., P. T. Metzger, and C. D. Immer (2008), Lagrangian trajectory modeling of lunar dust particles, paper presented at Earth and Space 2008, 11th Biennial Aerospace Division International Conference on Engineering, Construction and Operations in Challenging Environments, Am. Soc. of Civ. Eng., Long Beach, Calif.
- Lane, J. E., P. T. Metzger, and J. W. Carlson (2010), Lunar dust particles blown by lander engine exhaust in rarefied and compressible flow, paper presented at Earth and Space 2010, 12th Biennial Aerospace Division International Conference on Engineering, Construction and Operations in Challenging Environments, Am. Soc. of Civ. Eng., Honolulu, Hawaii.
- Lindsay, J. F. (1976), *Lunar Stratigraphy And Sedimentology*, *Dev. Solar Syst. Space Sci. Ser.*, vol. 3, edited by Z. Kopal and A. G. W. Cameron, pp. 232–237, Elsevier, New York.
- Lumpkin, F., J. Marichalar, and A. Piplica (2007), Plume impingement to the lunar surface: A challenging problem for DSMC, paper presented at Direct Simulation Monte Carlo Theory, Methods and Applications Conference, Sandia Natl. Lab., Santa Fe, N. M.
- Mason, C. C. (1970), Comparison of actual versus predicted lunar surface erosion caused by Apollo 11 descent engine, *Geol. Soc. Am. Bull.*, 81(6), 1807–1812, doi:10.1130/0016-7606(1970)81[1807:COAVPL]2.0.CO;2.
- Mason, C. C., and E. F. Nordmeyer (1969), An empirically derived erosion law and its application to lunar module landing, *Geol. Soc. Am. Bull.*, 80(9), 1783–1788, doi:10.1130/0016-7606(1969)80[1783:AEDELA]2.0.CO;2.
- McKay, D. S., and A. Basu (1983), The production curve for agglutinates in planetary regoliths, *Proc. 14th Lunar Planet. Sci. Conf., Part 1, J. Geophys. Res.*, 88, Suppl., B193–B199, doi:10.1029/JB088iS01p0B193.
- McKay, D. S., R. M. Fruland, and G. H. Heiken (1974), Grain size and the evolution of lunar soils, *Geochim. Cosmochim. Acta*, 1, 887–906.

- McKay, D. S., G. Heiken, A. Basu, G. Blanford, S. Simon, R. Reedy, B. M. French, and J. Papike (1991), The lunar regolith, in *Lunar Sourcebook, A User's Guide to the Moon*, edited by G. H. Heiken, D. T. Vaniman, and B. M. French, pp. 285–386, Cambridge Univ. Press, Melbourne, Australia.
- Mendell, W. W., and S. K. Noble (2010), The epiregolith, *Lunar Planet. Sci.*, 41st, Abstract 1348.
- Metzger, P. T., J. E. Lane, and C. D. Immer (2008), Modification of Roberts' theory for rocket exhaust plumes eroding lunar soil, paper presented at Earth and Space 2008, 11th Biennial Aerospace Division International Conference on Engineering, Construction and Operations in Challenging Environments, Am. Soc. of Civ. Eng., Long Beach, Calif.
- Metzger, P. T., C. D. Immer, C. M. Donahue, B. T. Vu, R. C. Latta III, and M. Deyo-Svendsen (2009a), Jet-induced cratering of a granular surface with application to lunar spaceports, *J. Aerosp. Eng.*, 22(1), 24–32, doi:10.1061/(ASCE)0893-1321(2009)22:1(24).
- Metzger, P. T., R. C. Latta III, J. M. Schuler, and C. D. Immer (2009b), Craters formed in granular beds by impinging jets of gas, in *Powders And Grains 2009: Proceedings Of The 6th International Conference on Micromechanics of Granular Media, AIP Conf. Proc. Ser.*, vol. 1145, edited by M. Nakagawa and S. Luding, pp. 767–770, Am. Inst. of Phys., Melville, N. Y., doi:10.1063/1.3180041.
- Metzger, P. T., J. E. Lane, C. D. Immer, and S. Clements (2010a), Cratering and Blowing Soil by Rocket Engines During Lunar Landings, in *Lunar Settlements, Adv. in Eng. Ser.*, edited by H. Benaroya, pp. 551–576, CRC Press, Boca Raton, FL, doi:10.1201/9781420083330-c38.
- Metzger, P. T., E. J. Lane, C. D. Immer, J. N. Gamsky, W. Hauslein, X. Li, R. C. Latta III, and C. M. Donahue (2010b), Scaling of erosion rate in subsonic jet experiments and Apollo lunar module landings, paper presented at Earth and Space 2010, 12th Biennial Aerospace Division International Conference on Engineering, Construction and Operations in Challenging Environments, Am. Soc. of Civ. Eng., Honolulu, Hawaii.
- Moore, H. J., R. E. Hutton, G. D. Clow, and C. R. Spitzer (1987), Physical properties of the surface materials at the Viking landing sites on Mars, *U.S. Geol. Surv. Prof. Pap.*, 1389, 35–44.
- Morris, B., D. B. Goldstein, P. L. Varghese, and L. M. Trafton (2010), Plume impingement on a dusty lunar surface, paper presented at 27th International Symposium on Rarefied Gas Dynamics, Pa. State Univ., Pacific Grove, Calif.
- NASA Manned Space Center (1969a), Apollo 11 technical air-to-ground voice transcription, pp. 316, 324, 377, and 427, Houston, Tex.
- NASA Manned Space Center (1969b), Apollo 11 technical debriefing v. 1 and 2, *Rep. MSC-276*, pp. 9.24–9.28, and 12.3–12.12, NASA Manned Space Cent., Houston, Tex.
- NASA Manned Space Center (1969c), Apollo 12 technical air-to-ground voice transcription, pp. 348, 409, 436, Houston, Tex.
- NASA Manned Space Center (1969d), Apollo 12 technical debriefing, *Rep. MSC-0255*, pp. 9.11–9.12, 9.15, 9.17, 10.25, and 12.1–12.2, Houston, Tex.
- NASA Manned Space Center (1971a), Apollo 14 technical air-to-ground voice transcription, pp. 381, 449–50.464–6, 582, Houston, Tex.
- NASA Manned Space Center (1971b), Apollo 14 technical debriefing, *Rep. MSC-310*, pp. 9.17–9.18, 10.20, and 12.1, Houston, Tex.
- NASA Manned Space Center (1971c), Apollo 15 technical air-to-ground voice transcription, *Rep. MSC-4558*, pp. 320, 371, 437, and 440, Houston, Tex.
- NASA Manned Space Center (1971d), Apollo 15 technical debriefing, *Rep. MSC-4561*, pp. 9–14, Houston, Tex.
- NASA Manned Space Center (1971e), Apollo 15 mission report, *Rep. MSC-05161*, pp. 62–63, Houston, Tex.
- NASA Manned Space Center (1972a), Apollo 16 technical air-to-ground voice transcription, *Rep. MSC-6802*, pp. 465–6, and 618–9, Houston, Tex.
- NASA Manned Space Center (1972b), Apollo 16 technical debriefing, *Rep. MSC-6805*, pp. 9.13, 10.25, and 10.33–10.34, Houston, Tex.
- NASA Manned Space Center (1972c), Apollo 17 technical air-to-ground voice transcription, *Rep. MSC-7629*, pp. 74A/15 and 77A/34, Houston, Tex.
- NASA Manned Space Center (1973), Apollo 17 technical debriefing, *Rep. MSC-7631*, pp. 9.7–9.8, Houston, Tex.
- O'Brien, B. J. (2009), Direct active measurements of movements of lunar dust: Rocket exhausts and natural effects contaminating and cleansing Apollo hardware on the Moon in 1969, *Geophys. Res. Lett.*, 36, L09201, doi:10.1029/2008GL037116.
- O'Brien, B. J., S. C. Freden, and J. R. Bates (1970), Degradation of Apollo 11 deployed instruments because of lunar module ascent effects, *J. Appl. Phys.*, 41(11), 4538–4541, doi:10.1063/1.1658493.
- Park, J., Y. Liu, K. D. Kihm, and L. A. Taylor (2008), Characterization of lunar dust for toxicological studies, part I: Particle size distribution, *J. Aerosp. Eng.*, 21(4), 266–271, doi:10.1061/(ASCE)0893-1321(2008)21:4(266).
- Phillips, P. G., et al. (1988), Lunar base launch and landing facility conceptual design, *NASA Contract NAS9-17878 Final Report, EEI Report 88-178*, Eagle Eng., Webster, Tex.
- Pieters, C. M., L. A. Taylor, S. K. Noble, L. P. Keller, B. Hapke, R. V. Morris, C. C. Allen, D. S. McKay, and S. Wentworth (2000), Space weathering on airless bodies: Resolving a mystery with lunar samples, *Meteorit. Planet. Sci.*, 35, 1101–1107, doi:10.1111/j.1945-5100.2000.tb01496.x.
- Roberts, L. (1963), The action of a hypersonic jet on a dust layer, paper 63-50 presented at 31st Annual Meeting, Inst. Aerosp. Sci., New York.
- Sabaroff, S. (1965), Sources and effects of electrical charge accumulation and dissipation on spacecraft, *IEEE Trans. Electromagn. Compat.*, 7(4), 437–444, doi:10.1109/TEMC.1965.4307439.
- Scott, R. F. (1975), Apollo Program Soil Mechanics Experiment, *NASA Conf. Rep., CR-144438*.
- Scott, R. F., and H.-Y. Ko (1968), Transient rocket-engine gas flow in soil, *AIAA J.*, 6(2), 258–264, doi:10.2514/3.4487.
- Shoemaker, E. M., R. M. Batson, H. E. Holt, E. C. Morris, J. J. Rennison, and E. A. Whitaker (1967), Television observations from Surveyor III, in *Surveyor III: A Preliminary Report, NASA Spec. Publ.*, SP-146, 43 pp.
- Taylor, L. A., C. M. Pieters, L. P. Keller, R. V. Morris, and D. S. McKay (2001), Lunar mare soils: Space weathering and the major effects of surface-correlated nanophase Fe, *J. Geophys. Res.*, 106(E11), 27,985–27,999, doi:10.1029/2000JE001402.
- Taylor, L. A., C. Pieters, A. Patchen, D.-H. Taylor, R. V. Morris, L. P. Keller, and D. S. McKay (2003), Mineralogical characterization of lunar highland soils, *Lunar Planet. Sci.*, XXXIV, Abstract 1774.
- Tosh, A., P. A. Liever, R. R. Arslanbekov, and S. D. Habchi (2011), Numerical analysis of spacecraft rocket plume impingement under lunar environment, *J. Spacecr. Rockets*, 48(1), 93–102, doi:10.2514/1.50813.
- Walton, O. R. (2007), Adhesion of lunar dust, *NASA Conf. Rep., CR-2007-214685*.
- Wright, V. Paul (1993), *Sedimentology Review*, 103 pp., Wiley-Blackwell, Oxford, U. K.
- Zeng, X., C. He, H. Oravec, A. Wilkinson, J. Agui, and V. Asnani (2010), Geotechnical properties of JSC-1A lunar soil simulant, *J. Aerosp. Eng.*, 23(2), 111–116, doi:10.1061/(ASCE)AS.1943-5525.0000014.

J. E. Lane, ASRC Aerospace, Kennedy Space Center, FL 32899, USA. (John.E.Lane@nasa.gov)

P. T. Metzger, Granular Mechanics and Regolith Operations Lab, NE-S-1, NASA Kennedy Space Center, FL 32899, USA. (Philip.T.Metzger@nasa.gov)

J. Smith, Pacific International Space Center for Exploration Systems, University of Hawaii at Hilo, 200 W. Kawili St., Hilo, HI 96720-4091, USA.